SPRAY POND MATHEMATICAL MODEL FOR COOLING FRESH WATER AND BRINE

By

ASEM M. ELGAWHARY

Bachelor of Science
Cairo University
Cairo, U. A. R.
June, 1963

Master of Science
Oklahoma State University
Stillwater, Oklahoma
August, 1969

Submitted to the Faculty of the Graduate College
of the Oklahoma State University
in partial fulfillment of the requirements
for the Degree of
DOCTOR OF PHILOSOPHY
July, 1971

SPRAY POND MATHEMATICAL MODEL FOR

COOLING FRESH WATER AND BRINE

Thesis Approved:

Allen M. Rowe
Thesis Adviser

Forrest D. Whitfield

W. A. Wiedeman, Jr.

J. A. Wiebelt

Joyce P. McDonald

D. Dunham
Dean of the Graduate College

ACKNOWLEDGEMENTS

The writer wishes to express his sincere appreciation and gratitude to the following individuals and organizations.

To Dr. Allen M. Rowe, Thesis Adviser and Chairman of the Advisory Committee, for his valuable counsel and continuous advice throughout this study; and to Drs. J. A. Wiebelt and W. G. Tiederman, members of the Advisory Committee for their sincere help and valuable suggestions throughout this investigation.

To Drs. F. C. McQuiston and F. D. Whitfield, members of the Advisory Committee, for their significant suggestions and expressed interest during the work.

To Dr. J. D. Parker for his instruction and his personal guidance.

To the United States Department of Interior, Office of Water Resources Research, for providing funds which helped to make this study financially possible.

To the School of Mechanical and Aero-Space Engineering for its financial support.

To Mrs. Margaret Estes for typing the manuscript.

TABLE OF CONTENTS

LIST OF TABLES

LIST OF FIGURES

NOMENCLATURE

C = Vapor concentration

C_i = Initial vapor concentration in the cell

$\overline{C}$ = Mean vapor concentration in the cell

C_o = Vapor concentration in equilibrium with the droplet

C_∞ = Vapor concentration in the cell boundary

C_p = Specific heat of the droplet fluid

C_s = Saturated vapor concentration in the cell

C_t = Vapor concentration in the cell at time t

D = Diffusion coefficient

DBT = Dry bulb temperature

e = The base of the natural system of logarithms 2.71828 . . .

h = Heat transfer coefficient

h_D = Mass transfer coefficient

I = Rate of droplet evaporation

k_a = Air thermal conductivity

k_w = Droplet fluid thermal conductivity

L = Latent heat of vaporization of droplet fluid

m = Mass of droplet

m_o = Initial mass of droplet

M = Molecular weight of droplet fluid in vapor case

P = Partial vapor pressure

P_o = Partial vapor pressure at droplet surface

P_s = Saturated partial vapor pressure at cell boundary

Pr = Prandtl number

r = Droplet radius at time t

r_o = Initial droplet radius

R = Cell radius

R_g = Gas constant

Re = Reynolds number

Y_i = Initial salt concentration

Y_t = Salt concentration after time t

$Y_m = (Y_i + Y_t)/2$

Sc = Schmidt number

t = Exposure time

t_s = Exposure saturation time

T = Droplet absolute temperature

$T_m = (T_o + T_t)/2$

T_o = Initial droplet absolute temperature

T_s = Absolute outlet saturation temperature

T_t = Absolute outlet temperature at time t

TDP_o = Thermodynamic properties at T_o

TDP_m = Thermodynamic properties at T_m

u = Relative velocity of the droplet

WBT = Wet bulb temperature

$\varkappa$ = Relative humidity

We = Weber number

ρ = Droplet fluid density

ρ_a = Air density

σ = Surface tension

δ = Tolerance factor

ν = Kinematic viscosity of the medium

ΔP = Nozzle pressure drop

CHAPTER I

INTRODUCTION

1.1 Discussion

Thermal changes in the aquatic environment are a naturally occurring phenomenon; but since World War II rapid and sometimes massive changes have been introduced by man. The capacity of the environment to absorb heat without suffering damage is limited and is being exceeded in many cases today [1]. Control of this heat disposal is essential for the protection of aquatic resources. Discharged cooling water is often 10 to 20°F warmer than the receiving water, while a three or four degree change can devastate the biota [1]. Both temperature levels and duration of those levels are critical.

Oxygen consumption by aquatic vertebrates doubles for every 18°F rise in stream temperature; but, as those temperatures rise, the water holds less oxygen in solution. Thus, while the supply of dissolved oxygen (DO) steadily dwindles with increased temperatures, the demand for DO increases. As a consequence ecologists have become more concerned with this problem of thermal pollution.

Thermal pollution primarily results when power plants and other such facilities withdraw water from streams, lakes, oceans, and rivers for cooling or condensing purposes, which is then returned to the water ways. Nearly all water withdrawn for industrial manufacturing plants and thermal electric utilities is for such cooling purposes. In 1964,

for example, 90 per cent of the total 48,900 billion gallons withdrawn by industry and investor-owned thermal-electric utilities, or about 44,200 billion gallons a year, was used for cooling and condensing purposes [1].

In a modern, coal-fired steam power plant, over one-half of the heat input must be dissipated by cooling water in heat exchangers. Nuclear plants are even less efficient, and require about 40 per cent more cooling water than coal-fired plants.

Today, about 70 per cent of the industrial thermal pollution load in the United States is caused by the steam-electric power industry. The other 30 per cent comes from the petroleum, chemical, steel, and paper processing industries. Concern over these damaging effects of thermal pollution is growing among many water users and at all levels of the government. Effective action was taken at the federal level in 1965 to control waste heat, as well as all other types of water pollutants. Congress passed the Water Quality Act of 1965, requiring water quality standards to be set and implemented for all interstate and coastal waters. The states first formulated these standards, which were submitted to the Department of the Interior by June 30, 1967, for review. Some standards have been approved at the federal level; others are under active review.

These standards specify desired beneficial uses for water and established criteria for protection; one of the criteria concerns water temperature. Waters of different types (warm, cold, and/or marine), designated for different uses (fish propagation, body contact sports, industrial, and/or municipal supply), are usually assigned different temperature limits. For example, warm water fisheries may have a $90^{\circ}F$

maximum; cold water (for salmonoids) may have a maximum temperature limit of 68°F, while trout streams may have a 65°F maximum.

The solution to problems created by thermal pollution fit generally into five categories:

1. means to minimize the effect of the waste heat on the aquatic environment,
2. means to reduce waste heat produced in thermal generation plants,
3. uses for waste heat,
4. methods to dispose of waste heat, and
5. new, non-polluting methods of power generation.

This work proposes a study concerned with the fourth category dealing with reducing the water temperature associated with waste heat disposal. Methods now in use to control cooling water temperature include evaporative cooling towers, non-evaporating cooling systems, air cooling, and cooling ponds or spray ponds. In particular this study is concerned with the analysis of the later system--the spray pond.

1.2 Spray System

One of the most significant advantages of a spray pond is that besides providing cooling it also increases the amount of air dissolved in the water. This dissolved air provides oxygen for the aquatic vertebrates and helps bacteria to decompose pollutants.

The hot discharge water or brine can be cooled by spraying it into a stream of outside air. A very small portion of the warm water or warm brine is evaporated upon contact with the air. The heat required to vaporize the water comes from the hot water or brine, thereby

reducing its temperature. The lowest temperature to which water or brine can be cooled by an atmospheric device is the wet-bulb temperature of the entering air. Performance is frequently specified in terms of approach of the leaving-water temperature to the entering-air wet-bulb temperature for a particular cooling range, defined as the temperature decrease of the water. The cooling efficiency of any atmospheric water cooling equipment relates the wet-bulb temperature to the cooling range by the following equation,

$$E \equiv \frac{t_{iw} - t_{ow}}{t_{iw} - t'} \times 100 \qquad (1.1)$$

where

E = efficiency (per cent),

t_{iw} = temperature of inlet water $^{\circ}F$,

t_{ow} = temperature of outlet water $^{\circ}F$, and

t' = wet-bulb temperature of entering air $^{\circ}F$.

CHAPTER II

DEFINITION OF THE PROBLEM

The objective of this work is to systematically analyze the spray pond cooling method in order to establish design criterion for engineering and economic evaluation of spray cooling for a wide variety of prevailing atmospheric conditions.

Most of the theoretical works on spray systems have been associated with the problems of spray combustion in rocket engines and spray drying in closed containers [2]. In these studies it has been assumed that the spray system is confined in a closed vessel and no consideration has been given to factors often encountered under atmospheric conditions such as mass diffusion from the droplet and temperature change due to evaporation.

A literature survey revealed that only one technique has been published concerned with the design of spray ponds [3]. This work was entirely empirical; the only independent variables considered were the ambient wet-bulb temperature, the wind velocity, water flow rate through the nozzle, and initial water temperature.

The model proposed here is based on energy and mass balance equations as well as established empirical relations, and involves the following independent variables:

1. wet and dry bulb temperature,
2. initial drop size and air volume per droplet,

3. exposure time per droplet,

4. wind velocity,

5. brine concentration,

6. initial temperature of input water or brine, and

7. number of stages of the spray pond system.

The development of this model is necessary in order to evaluate to what extent each of these variables effects spray pond performance.

In this study the cellular model was used in analyzing the spray system. This model is readily adaptable to various circumstances in which atmospheric conditions and droplet dynamics play important roles.

By studying weather data for a given area, engineers will then be able to use the model developed in this study to design a cooling system to reduce thermal pollution caused by the discharge of cooling water of power plants or the discharge of brine of desalting plants.

CHAPTER III

PLAN OF ATTACK

Energy and mass balance equations were applied to the spray system in formulating a mathematical model to calculate the decrease in temperature of either water or brine by spray cooling.

The cooling and evaporation that occurs by spraying water or brine droplets into a gaseous media (air) is extremely complex. The process is non-stationary and occurs in a medium with unequal temperature and vapor distributions. The drops move irregularly relative to the medium and are more or less deformed, while circulation occurs within the droplets; heat transfer between the drops and the medium occurs by three different mechanisms (conduction, convection, and radiation). The exact solution to this problem is, therefore, very complex and a number of simplifying assumptions were made in order to solve this problem.

3.1 Basic Assumptions

1. The cellular model was used to analyze the multi-droplet system. This model divides the spray under consideration into a number of identical cells, one droplet occupying each cell. The problem is thus reduced to the consideration of a single droplet and its boundary envelope. Thus, the spray under consideration can be imagined as formed of a series of cubes, each containing

a droplet in its center. This cube was replaced by an equivalent sphere of radius R as shown in Figure 1.

2. For simplicity, it was assumed that all droplets were spherical, of the same size, and equidistance from each other by a distance 2R.

3. Furthermore, it was assumed there would be no effective mass transfer between cells. Basically, two mechanisms would contribute to such a transfer for droplets with a radius less than one micron; difference in droplet surface tension, and/or difference in saturation pressure. A difference in surface tension would effect the diffusion coefficient, while a difference in saturation pressure would result in a concentration gradient across the cell boundary. However, these effects are not observed for droplets greater than one micron which represent the size of droplets of this problem [4].

4. At the edge of each cell, the vapor concentration, C_{∞}, was considered quasiconstant and approximately equal to the average concentration, $\bar{C}(t)$, in the spray system at time t. This assumption seems reasonable if one examines the concentration distribution around a droplet given in Figure 2 [2].

5. Evaporation stops when the cell becomes saturated with water vapor.

6. The atmospheric conditions (relative humidity, dry bulb temperature) at the nozzle were assumed to be the same as the prevailing weather conditions.

7. Since the partial pressure of the vapor in the spray system is relatively small, it was assumed that the vapor obeys the ideal

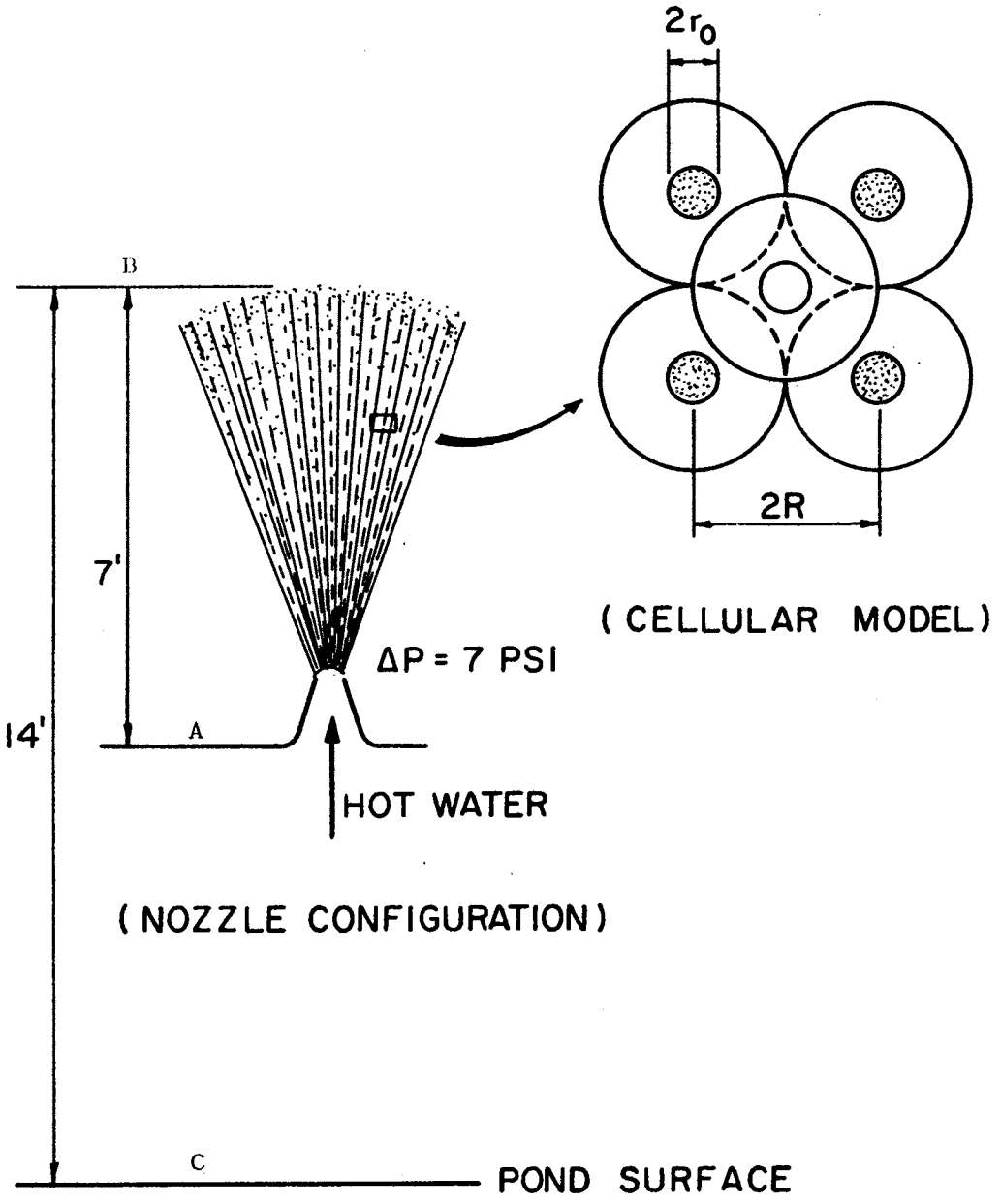

Figure 1. Spray Model

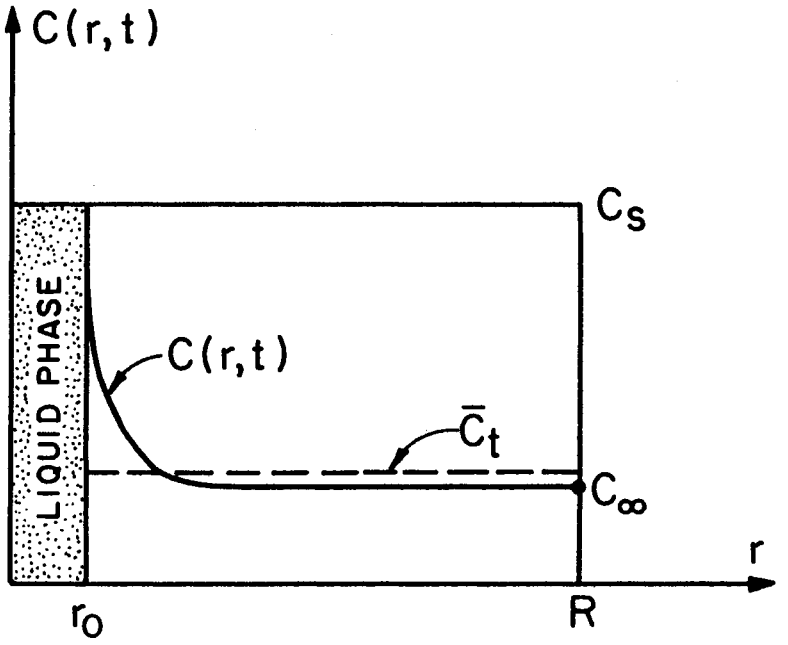

Figure 2. Concentration Distribution Around a Droplet in a Concentric Spherical Vessel with Nonabsorbing Wall

gas law.

8. The air entrained in the spray moves with each droplet as it travels from the nozzle to the pond's surface.
9. Horizontal displacement of vapor between adjacent cells due to wind velocity does not result in a change in vapor properties.

3.2 Proposed Solution

At small Reynolds number ($Re \ll 1$), the cooling and evaporation of droplets moving relative to the medium does not differ significantly from the case of a droplet which is motionless relative to the medium. This conclusion is based on the fact that the concentration and temperature distribution around the droplet are disturbed very little by the droplet's movement. Fluid circulation within the droplet, caused by friction against the gaseous medium, which helps to equalize the temperature within the droplets, has no important effect at low Reynolds number.

At larger Reynolds numbers ($Re > 1$), diffusion and heat transfer are localized in a thin boundary layer and the relaxation time of the temperature and concentration distribution at a given surface temperature have a value of the order (ν/u^2). The time for internal temperature relaxation of the droplets is considerably less than for motionless droplets due to fluid circulation in the droplets. Hence, the non-stationary cooling and evaporation of droplets moving relative to the medium does not differ significantly from a quasi-stationary cooling and evaporation of droplets moving relative to the medium. This latter case can be solved with relative ease.

3.3 Proposed Mathematical Models

Energy and mass balance equations were applied to the droplet in formulating a mathematical model to calculate the decrease in temperture by spray cooling either water or brine.

3.3.1 The Energy Balance Equation

The Biot number $\left(Bo = \frac{hl}{k}\right)$ is used to compare the relative magnitudes of internal and external resistance to heat transfer. For relatively small values of the Biot number, the droplet can be considered to be nearly at a uniform temperature at all times. This would be the case where the internal resistance is negligible compared to the external resistance.

For a water or brine droplet ($k = 0.363$ BTU/hr ft°F) of 0.1875" diameter cooled by forced convection in air $\left[h \simeq \frac{k_a}{r_o}(1 + 0.3\, Re^{1/2} Pr^{1/3}),\right.$ using Ranz and Marshall's equation [5]$\left.\right]$, the Biot number is 0.19 for a value of the Reynolds number equal to 800. This value of Biot number is relatively small, which implies a uniform temperature exists in the droplet.

Since the droplets have uniform temperatures, the energy balance equation applied to the droplet yields the following expression:

$$L\, I\, dt + h\, 4\pi r_o^2 (T_o - T_\infty) dt = -C_p\, \rho \frac{4}{3} \pi\, r_o^3\, dT \qquad (3.1)$$

where,

t = time,

T = temperature,

L = latent heat of water or brine,

I = rate of evaporation of droplet,

h = heat transfer coefficient,

r_o = droplet radius,

T_o = droplet temperature at radius r_o,

T_∞ = medium temperature at radius R,

C_p = specific heat of the brine droplet, and

ρ = droplet density.

The first term $[L\ I\ dt]$ expresses the quantity of heat required to evaporate water from the droplet, while the second term $[h\ 4\pi r_o^2\ (T_o - T_\infty) dt]$, is the amount of heat received by the medium from the droplet by potential gradients (as in simple conduction) and by movement of the fluid in the medium itself. The heat received by the medium from the droplet by radiation was considered negligible. The last term $[C_p\ \rho\ \frac{4}{3}\pi r_o^3\ dT]$, represents the change in the enthalpy of the droplet.

In order to solve the energy balance equation, one needs to determine the rate of evaporation, I, with the diffusion equation which is derived in Appendix D.

3.3.2 The Mass Balance Equation

Evaporation occurs until the cell becomes saturated. At this time evaporation ceases, and the first term in the energy balance equation becomes zero. This saturation time, t_s, was determined from the mass balance equation as follows.

At any given time, the mass lost by the droplet must be equal to the mass gained by the gas medium (air), and results in the following mass balance equation:

$$m_o - m = \frac{4}{3}\rho\pi(r_o^3 - r^3) \tag{3.2}$$

$$= \int_r^R 4\pi r^2 C dr - \frac{4}{3}\pi C_i(R^3 - r_o^3)$$

$$= \frac{4}{3}\pi\bar{C}(R^3 - r^3) - \frac{4}{3}\pi C_i(R^3 - r_o^3) \tag{3.3}$$

where,

ρ = droplet density,

m_o = initial mass of the droplet,

r_o = initial radius of the droplet, and

C_i = initial concentration of the medium.

The average concentration, $\bar{C}$, is defined by the following equation [2]:

$$\bar{C}(t) = \frac{\int_r^R C(r,t)4\pi r^2 dr}{\frac{4}{3}\pi(R^3 - r^3)} . \tag{3.4}$$

The droplet radius decreased as evaporation occurs. Under steady state conditions, the rate of change of droplet radius can be determined from the following equation:

$$I = -\frac{dm}{dt} . \tag{3.5}$$

By integrating the energy balance equation, using the mass balance equation results, the decrease in the temperature of the droplet can be determined as outlined in Chapter IV.

3.3.3 The Rate of Evaporation

The rate of evaporation at small and large values of Reynolds number is given by the following equations

$$I = 4\pi r_o D(C_o - C_\infty) \tag{3.6}$$

$$Re \ll 1$$

and

$$I = 4\pi r_o D(1 + 0.3\ Re^{1/2}\ Sc^{1/3})(C_o - C_\infty) \tag{3.7}$$

$$R > 1 \ .$$

These equations result from the solution of the diffusion equations with their appropriate boundary and initial conditions as shown in Appendix D.

3.3.4 Heat and Mass Transfer Coefficients

In order to solve the energy and mass balance equations, heat and mass transfer coefficients have to be determined. The heat and mass transfer coefficients at small values of Reynolds number ($Re \ll 1$) assume values corresponding to a zero relative velocity (still air).

At large values of Reynolds number ($Re > 1$), following the majority of the workers in this field, it has been assumed that convection effects can be evaluated by using Ranz and Marshall's equation [5], for which heat and mass transfer coefficients were expressed as function of the Reynolds number, Schmidt number, and Prandtl number. The average values of these coefficients are given by the following equations:

$$h_{average} = h_{still\ air}\ [1 + 0.3(Re)^{1/2}(Pr)^{1/3}] \tag{3.8}$$

$$h_{D_{average}} = h_{D_{still\ air}}\ [1 + 0.3(Re)^{1/2}(Sc)^{1/3}] \tag{3.9}$$

where,

$$h_{still\ air} = \frac{k_a}{r_o} \ ,$$

$$h_{D_{\text{still air}}} = \frac{D}{r_o} \quad ,$$

Re = Reynolds number,

Pr = Prandtl number, and

Sc = Schmidt number.

3.3.5 Drop Size

In order to solve the energy and mass balance equations, the initial drop size has to be determined. A thorough literature survey revealed that all the data available relating the orifice and droplet diameters for spraying water are for relatively high pressure drops, of the order of 50 psi and more [6]. At 50 psi, the average drop diameter is of order seven to nine per cent of 0.063" orifice diameter for a hollow-cone nozzle [6]; the type used in spray ponds. However, the rate of flow and the orifice diameters presented in reference [6] are low compared to values for spray pond nozzles.

Studies on the drop size from pressure nozzles for spraying fuel have been conducted that involve nozzle pressure drops in a range applicable to spray ponds. Longwell proposed a correlation for the mean drop size, which has been reported by Marshall [7] as follows:

$$D_o = \frac{D_{or}\, k_L\, e^{0.705\nu}}{2\, P_n^{0.375} (\sin \theta/2)} \qquad (3.10)$$

where,

D_o = droplet mean diameter,

D_{or} = orifice diameter,

k_L = constant = 0.72 for fuel oil,

ν = kinematic viscosity, stokes,

P_n = nozzle pressure, lb/sq.in., and

θ = spray-cone angle.

Since there was no data available to determine the best value for k_L for water and brine, calculations were performed for both water and brine using the k_L value reported for fuel oil to estimate droplet size.

The results are summarized below for a pressure drop of 7 psi, and $\theta = 72^{\circ}$ for different orifice diameters:

orifice diameter	11/16"	1"	1 5/16"
droplet diameter	0.125"	0.1875"	0.25"
$We = \rho_a \frac{u^2 D_o}{\sigma}$	5.2	8.3	11

where,

ρ_a = air density, lbm/ft^3,

u = relative velocity between liquid and air, ft/sec, and

σ = surface tension, $lbm\ ft/sec^2 ft$.

For values of the Weber number, We, less than 20, the droplets are stable and will not break into smaller droplets [8].

3.3.6 Thermodynamic Properties

One object of this study was to analyze spray cooling of brine. In order to perform this analysis, the thermodynamic properties were established as a function of temperature and salt concentration and are tabulated below:

A. Vapor Pressure [9]

i. Fresh Water

$$\ln P_{water} = 71.02449 - \frac{7381.6477}{T} - 9.0993037 \ln T + 0.0070831558\ T \qquad (3.11)$$

where,

P_{water} = vapor pressure of fresh water, atm, and

T = temperature, degrees Kelvin.

ii. Aqueous Sodium Chloride Solutions

$$\ln P_{solution} = A(Y) \times \ln P_{water} + B(Y) \tag{3.12}$$

where,

$P_{solution}$ = vapor pressure of the solution, atm,

$A(Y) = 1 - 0.061430798\ Y + 1.2470136\ Y^2$,

$B(Y) = Y(2.027886 - 1.4908968\ Y + 77.008083\ Y^2)$, and

Y = the mole fraction of salt contained in the solution.

B. Specific Volume [10]

$$V = A(T) + Y \times D(T) + Y^2 \times E(T) \tag{3.13}$$

where,

V = specific volume, cm^3/gm,

T = temperature degrees Kelvin,

Y = the mole fraction of salt contained in the solution,

$$A(T) = 5.9163665 - 0.1035794\ T + 0.9270048 \times 10^{-5}\ T^2 - \frac{1127.522}{T} + \frac{100674.1}{T^2},$$

$$D(T) = -2.5166 + 0.0111766\ T - 0.170552 \times 10^{-4}\ T^2, \text{ and}$$

$$E(T) = 2.84851 - 0.0154305\ T + 0.223982 \times 10^{-4}\ T^2.$$

C. Specific Heat [9]

$$C_p = 1.3041791 - 8.1519942\ Y + 16.203997\ Y^2 - (0.19159475 \times 10^{-2} - 0.029952864\ Y + 0.0037589577\ Y^2)T + (0.2994476 \times 10^{-5} - 0.498581 \times 10^{-4}\ Y - 0.89329066 \times 10^{-6}\ Y^2)T^2 \tag{3.14}$$

where,

C_p = specific heat, cal/deg°C,

T = temperature, degrees Kelvin, and

Y = the mole fraction of salt contained in the solution.

D. Heat of Vaporization

The best curve fit of Chou's [9] data of the heat of vaporization is used for the model calculation. The heat of vaporization of various percentages of salt concentrations, and temperature ranging from 32 to 350°F, are expressed by the following relationships:

For fresh water,

$$h_{f_g} = 1093.3258 - 0.57909483\ t + 0.228937 \times 10^{-3}\ t_1^2 - 0.1113056 \times 10^{-5}\ t_1^2 . \quad (3.15)$$

For 1 gm/100 gm solution salt concentration,

$$h_{f_g} = 1357.236 - 0.5276059\ T . \quad (3.16)$$

For 5 gm/100 gm solution salt concentration,

$$h_{f_g} = 1307.757 - 0.6729801\ T + 0.766083 \times 10^{-3}\ T^2 - 0.7675276 \times 10^{-6}\ T^3 . \quad (3.17)$$

For 10 gm/100 gm solution salt concentration,

$$h_{f_g} = 1434.863 - 1.15446\ T + 0.1282039 \times 10^{-2}\ T^2 - 0.8799693 \times 10^{-6}\ T^3 . \quad (3.18)$$

For 15 gm/100 gm solution salt concentration,

$$h_{f_g} = 1614.396 - 2.344322\ T + 0.3755414 \times 10^{-2}\ T^2 - 0.252578 \times 10^{-5}\ T^3 . \quad (3.19)$$

For 20 gm/100 gm solution salt concentration,

$$h_{f_g} = 1328.325 - 0.5227878\ T\ . \tag{3.20}$$

For 25 gm/100 gm solution salt concentration,

$$h_{f_g} = 1227.726 - 0.2038872\ T - 0.2457455 \times 10^{-3}\ T^2 \tag{3.21}$$

where,

h_{f_g} = heat vaporization, BTU/lbm,

t_1 = temperature, degrees Fahrenheit, and

T = temperature, degrees Rankine.

E. Mass Diffusivity [11]

$$D = \left(\frac{T}{273.2}\right)^{1.75} \times 0.22 \tag{3.22}$$

where,

D = mass diffusivity of water vapor to air, cm^2/sec, and

T = temperature, degrees Kelvin.

CHAPTER IV

FORMULATION OF SOLUTION

This chapter presents the derivations of equations relating the parameters t_s, T_s, and T_t for different ranges of Reynolds number (Re $\ll$ 1, and Re $>$ 1). These derivations are based on energy and mass balance equations, which have been discussed previously in Chapter III. Chapter V discusses how the equations developed in this chapter were used to calculate spray pond performance.

4.1 Solution for Low Values of the Reynolds Number, Re $\ll$ 1--Unsaturated Case

In this section equations are derived for very small values of wind velocity.

4.1.1 Determination of the Saturation Time, t_s

At any instant, the mass lost by a droplet must be equal to the mass gained by the gas medium, thus the mass balance equation becomes

$$m - m_o = \frac{4}{3}\pi\rho(r_o^3 - r^3)$$

$$= \frac{4}{3}\pi\bar{C}(R^3 - r^3) - \frac{4}{3}\pi C_i(R^3 - r_o^3) \qquad (4.1)$$

where the average vapor concentration in the spray system at any time t is evaluated with Equations (3.2) and (3.3), and found to be

$$\bar{C}(t) = \frac{\rho(r_o^3 - r^3) + C_i(R^3 - r_o^3)}{R^3 - r^3} . \qquad (4.2)$$

The radius of the droplet at time t is thus found to be related to $\bar{C}(t)$ by the expression,

$$r = \left[\frac{\rho(r_o^3 - \bar{C}R^3) + C_i(R^3 - r_o^3)}{\rho - \bar{C}}\right]^{1/3} . \qquad (4.3)$$

The droplet radius at saturation, r_s, is found by equating $\bar{C}(t)$ to the saturation concentration, C_s.

$$r_s = \left[\frac{(\rho r_o^3 - C_s R^3) + \varkappa C_s(R^3 - r_o^3)}{\rho - C_s}\right]^{1/3} \qquad (4.4)$$

where,

$C_i = \varkappa \times C_s$,

$\varkappa$ = relative humidity of the atmosphere, and

C_s = the saturation concentration.

The droplet radius decreases as evaporation occurs. For a constant rate of mass change (see Appendix D for justification), the rate of change of droplet radius can be determined from the following equation:

$$I = -\frac{dm}{dt} \qquad (4.5)$$

where,

$m = \frac{4}{3}\rho\pi r^3$, and

$I = 4\pi r D(C_o - C_\infty)$.

Therefore,

$$-r\frac{dr}{dt} = \frac{D}{\rho}(C_o - C_\infty) . \qquad (4.6)$$

As stated in Section 3.1, at the edge of each cell, the vapor concentration, C_∞, was considered quasi-constant and approximately equal to the average concentration, $\bar{C}(t)$, in the spray system at time t. Thus, using Equation (4.2), Equation (4.6) becomes

$$dt = \frac{r\rho}{D}\left[\frac{R^3 - r^3}{A - Br^3}\right]dr \tag{4.7}$$

where,

$A = (\rho r_o^3 - C_o R^3) + \varkappa \times C_s(R^3 - r_o^3)$, and

$B = (\rho - C_o)$.

Integrating Equation (4.7) from r_o to r_s and from t = 0 to t_s, where t_s is the time required to saturate the cell with water vapor, yields:

$$t_s = \frac{\rho}{D}\left(\frac{r_s^2 - r_o^2}{2B}\right) + \frac{\rho}{D}(R^3 - \gamma)\left[\frac{1}{3B(\gamma)^{1/3}}\right]$$

$$\times \left\{\frac{1}{2}\ln - \frac{\left[(\gamma)^{2/3} + (\gamma)^{1/3} r_s + r_s^2\right]\left[r_o - (\gamma)^{1/3}\right]^2}{\left[(\gamma)^{2/3} + (\gamma)^{1/3} r_o + r_o^2\right]\left[r_s - (\gamma)^{1/3}\right]^2}\right.$$

$$\left. + \sqrt{3}\tan^{-1}\left[\frac{2r_o + (\gamma)^{1/3}}{(\gamma)^{1/3}\sqrt{3}}\right] - \sqrt{3}\tan^{-1}\left[\frac{2r_s + (\gamma)^{1/3}}{(\gamma)^{1/3}\sqrt{3}}\right]\right\} \tag{4.8}$$

where,

$$\gamma = \frac{A}{B}\ .$$

4.1.2 Decrease in Spray Temperature

Substituting Equation (3.6) into Equation (3.1), the energy balance equation becomes:

$$4\pi r_o DL(C_o - C_t)dt + \frac{k_a}{r_o}\ 4\pi r_o^2\ (T_o - T_\infty)dt = -\ C_p\ \rho\frac{4}{3}\pi r_o^3\ dT\ . \tag{4.9}$$

Since the partial pressure of the vapor in the spray system is relatively small, it was assumed that the vapor obeys the ideal gas laws. Vapor concentration can then be expressed in terms of the vapor pressure.

$$C = \frac{PM}{R_g T} \tag{4.10}$$

where,

M = molecular weight of the evaporating substance in its gaseous form, and

R_g = universal gas constant.

Let P_s be the saturated vapor pressure at temperature T_∞, then

$$\frac{C_o}{C_s} \simeq \frac{P_o}{P_s} \simeq \mathrm{Exp}\left(-\frac{LM}{R_g}\frac{T_\infty - T_o}{T_\infty^2}\right) \tag{4.11}$$

which is the Clausis-Clapeyron equation, where,

L = latent heat of evaporating substance.

Substituting Equation (4.11) into the energy balance equation, Equation (4.9) becomes

$$(4\pi r_o D L C_s)\left[\mathrm{Exp}\left(\frac{LM}{R_g}\frac{T_o - T_\infty}{T_\infty^2}\right) - \varkappa\right]dt$$

$$+ \left(\frac{2k_a}{D_o}\right)(4\pi r_o^2)(T_o - T_\infty)dt = -C_p \rho \frac{4}{3}\pi r_o^3\, dT. \tag{4.12}$$

Now, by introducing the following two fundamental dimensionless quantities

$$\frac{T_o - T_\infty}{T_\infty^2}\frac{LM}{R_g} = Z \tag{4.13}$$

and

$$\frac{L^2 MDC_s}{k_a R_g T_\infty^2} = Q \qquad (4.14)$$

where,

C_s = the saturation concentration at T_∞,

Equation (4.12) becomes

$$LDC_s\left[Exp(Z) - \varkappa + \frac{Z}{Q}\right]dt = - C_p \frac{\rho r_o^2}{3} dT \ . \qquad (4.15)$$

Integrating Equation (4.15) results in temperature as function of time, for the case where the evaporation occurs.

Time t_s, is the time required for the cell to become saturated with water vapor. Therefore, Equation (4.15) becomes

$$t_s = - \frac{C_p \rho r_o^2}{3 Q k_a} \int_{Z_o}^{Z_s} \frac{\frac{1}{e}}{Exp(Z-1) + \frac{Z}{Qe} - \frac{1}{e}} dZ \qquad (4.16)$$

where,

$$Z_o = \frac{T_o - T_\infty}{T_\infty^2} \times \frac{LM}{R_g} \ ,$$

$$Z_s = \frac{T_s - T_\infty}{T_\infty^2} \times \frac{LM}{R_g} \ , \text{ and}$$

T_s = the droplet temperature at time t_s.

The highest value of Z is about 1.4 for water vapor at zero exposure time. Hence, as an approximation, the exponential term may be expanded in a power series, and only the first two terms need be considered for integration.

Thus,

$$T_s = T_\infty + \frac{R_g T_\infty^2}{LM\left(e + \frac{1}{Q}\right)} \times \left\{1 + \left[Z_o\left(e + \frac{1}{Q}\right) - 1\right] \times \text{Exp}\left[-\frac{3Q k_a \left(e + \frac{1}{Q}\right)}{C_p \rho r_o^2} t_s\right]\right\} . \quad (4.17)$$

4.2 Solution for Large Values of the Reynolds Number Re > 1--Unsaturated Case

In this section equations are derived that can be used to evaluate the effect of wind velocity on droplet temperature.

4.2.1 Determination of Saturation Time, t_s

The droplet radius decreases as evaporation occurs under steady state conditions, the rate of change of droplet radius can be directly determined from the equation

$$I \equiv -\frac{dm}{dt} \quad (4.18)$$

where,

$m = \frac{4}{3}\pi \rho r^3$,

$I = 4\pi r D' (C_o - C_\infty)$, and

$D' = D[1 + 0.3\ Re^{1/2}\ Sc^{1/3}]$ as shown in Appendix D.

Following the same procedure presented in Section 4.1, the exposure time, t_s, which is required to reach the saturation point in the cell is given by:

$$t_s = \frac{\rho}{D'}\left(\frac{r_s^2 - r_o^2}{2B}\right) + \frac{\rho}{D'}(R^3 - \gamma)\left[\frac{1}{3B(\gamma)^{1/3}}\right]$$

$$\times \left\{\frac{1}{2} \ln \frac{\left[\gamma^{2/3} + \gamma^{1/3} r_s + r_s^2\right]\left[r_o - \gamma^{1/3}\right]^2}{\left[\gamma^{2/3} + \gamma^{1/3} r_o + r_o^2\right]\left[r_s - \gamma^{1/3}\right]^2}\right.$$

$$\left. + \sqrt{3} \tan^{-1}\left[\frac{2r_o + \gamma^{1/3}}{\sqrt{3}\,\gamma^{1/3}}\right] - \sqrt{3} \tan^{-1}\left[\frac{2r_s + \gamma^{1/3}}{\sqrt{3}\,\gamma^{1/3}}\right]\right\} . \qquad (4.19)$$

In deriving Equation (4.19), it was assumed that, the change in Reynolds number, Re, is very small since the change in droplet radius is quite small.

4.2.2 Decrease in Spray Temperature

Ranz and Marshall's [5] equations for the heat and mass transfer coefficients (Equations (3.8) and (3.9)) were used for determining the decrease in spray temperature for Re > 1.

Following the same procedure presented in Section (4.1) the droplet temperature is given by:

$$T_s = T_\infty + \frac{R_g T_\infty^2}{LM\left(e + \frac{1}{Q_g}\right)} \times \left\{1 + \left[Z_o\left(e + \frac{1}{Q_g}\right) - 1\right]\right.$$

$$\left. \times \mathrm{Exp}\left[\frac{-3 Q_g k_a (1 + 0.3\ \mathrm{Re}^{1/2}\ \mathrm{Pr}^{1/3})\left(e + \frac{1}{Q_g}\right) t_s}{C_p \rho r_o^2}\right]\right\} \qquad (4.20)$$

where,

$$Q_g = Q \times \left[\frac{1 + 0.3\ \mathrm{Re}^{1/2}\ \mathrm{Sc}^{1/3}}{1 + 0.3\ \mathrm{Re}^{1/2}\ \mathrm{Pr}^{1/3}}\right] .$$

It is to be noted that Equations (4.19) and (4.20) will reduce to Equations (4.8) and (4.17), for a value of the Reynolds number equal to zero.

4.3 Decrease in Spray Temperature After the Cell Becomes Saturated

Evaporation stops when saturation occurs, then the first term of the energy balance equation, Equation (3.1), becomes zero. Thus, the energy balance equation becomes,

$$(h)(4\pi r_s^2)(T_s - T_\infty)dt = - C_p \rho \left(\frac{4}{3}\pi r_s^3\right)dT_s \quad . \tag{4.21}$$

Integration leads to the following equations for the pond temperature after saturation:

$$T_t = T_\infty + (T_s - T_\infty)\mathrm{Exp}\left[\frac{-3k_a(t - t_s)}{C_p \rho r_s^2}\right] \tag{4.22}$$

for $Re \ll 1$

and

$$T_t = T_\infty + (T_s - T_\infty)\mathrm{Exp}\left[\frac{-3k_a(1 + 0.3\ Re^{1/2}Pr^{1/3})(t - t_s)}{C_p \rho r_s^2}\right] \tag{4.23}$$

for $Re > 1$.

Equation (4.23) will reduce to Equation (4.22), for a value of the Reynolds number equal to zero.

CHAPTER V

CALCULATION PROCEDURE

5.1 Steps of Calculation

First the droplet free fall time was determined from the time a droplet leaves the nozzle until it strikes the surface of the pond. Next, the mass balance equation was used to determine the time required to saturate the cell with water vapor. Different forms of the energy balance were used to determine the final droplet temperature, depending on the comparison of saturation time to the free fall time, and on the Reynolds number. The Reynolds number was calculated using the wind velocity and the droplet diameter as parameters. The exact procedure followed is outlined below.

5.1.1 Total Exposure Time

The water leaving a spray nozzle will rise to a height of approximately one foot per psi nozzle pressure [12]. In a conventional upspray system, the elevation of the nozzles above the surface is 7 feet and the pressure drop across is 7 psi [12]. Therefore, the exposure time will be equal to the time taken by the water spray to reach an elevation of 7 feet and then return to the pond surface 7 feet below the nozzle level as shown in Figure 1. This time was determined by using uniformally accelerating motion assuming zero drag as a result of air entrainment. It was determined as follows:

From level A to level B,

$$S_u = V_o t_u + \tfrac{1}{2} g t_u^2 , \tag{5.1}$$

$$V = V_o + g t_u , \tag{5.2}$$

where,

S_u = spray travel distance from level A to level B,

V_o = initial velocity of the spray,

t_u = exposure time from level A to level B,

V = final velocity of the spray at level B, and

g = acceleration due to gravity,

hence,

$$t_u = \sqrt{\frac{2S_u}{g}} . \tag{5.3}$$

The spray velocity at level B is zero. Hence, from level B to level C Equation (5.1) becomes,

$$S_d = \tfrac{1}{2} g t_d^2 \tag{5.4}$$

where

S_d = spray travel distance from level B to level C, and

t_d = exposure time from level B to level C,

then,

$$t_d = \sqrt{\frac{2S_d}{g}} \tag{5.5}$$

$$t = t_u + t_d \tag{5.6}$$

where

t = the total exposure time.

5.1.2 The Saturation Time

The spray droplets will stop evaporating once the surrounding vapor pressure reaches the saturation pressure; r_s becomes the radius of the droplets at this saturation point. The time needed for the droplet radius to change from r_o to r_s is given by Equations (4.8) and (4.19).

5.1.3 The Outlet Temperature

For the case when the total exposure time is less than the required saturation time, either Equation (4.17) or Equation (4.20) was used to determine the final temperature, depending on the Reynolds number. However, if the total exposure time, t, was greater than the saturated time, t_s, either Equation (4.22) or Equation (4.23) was used to determine the additional change in temperature before the droplet strikes the pond's surface.

It was first assumed in the calculation that the thermodynamic properties of the droplet were constant at the initial temperature and salt concentration. Final temperature and salt concentration were thus determined. From the initial and final states so determined, average values of the thermodynamic properties were then used in the second solution to the problem. Repeated solutions were thus calculated until the properties from successive steps agreed to within 1%.

Temperature has no significant effect on Prandtl number and Schmidt number for water vapor under normal atmospheric conditions [13]. Hence, the value of 0.7 was assumed for both Prandtl number and Schmidt number in the model calculation.

5.2 Computer Program

A computer program was written to calculate the results presented in this study using the equations and procedure developed and discussed in Sections 4.1 through 5.1. The program was used to predict cooling for both fresh water and brine solutions by incorporating the effect of salt concentration on vapor pressure, specific volume, specific heat, and heat of vaporization for fresh and salt water. A detailed flow chart, indicating the step by step calculation, is presented in Figure 3.

The equations derived and used in the program were for Reynolds numbers equal to zero and greater than one. The Reynolds number range from zero to one was not evaluated in this study. However, should the Reynolds number fall in this range, Equation (D.14), Appendix D, can be used with the Prandtl number replacing the Schmidt number for the heat transfer case.

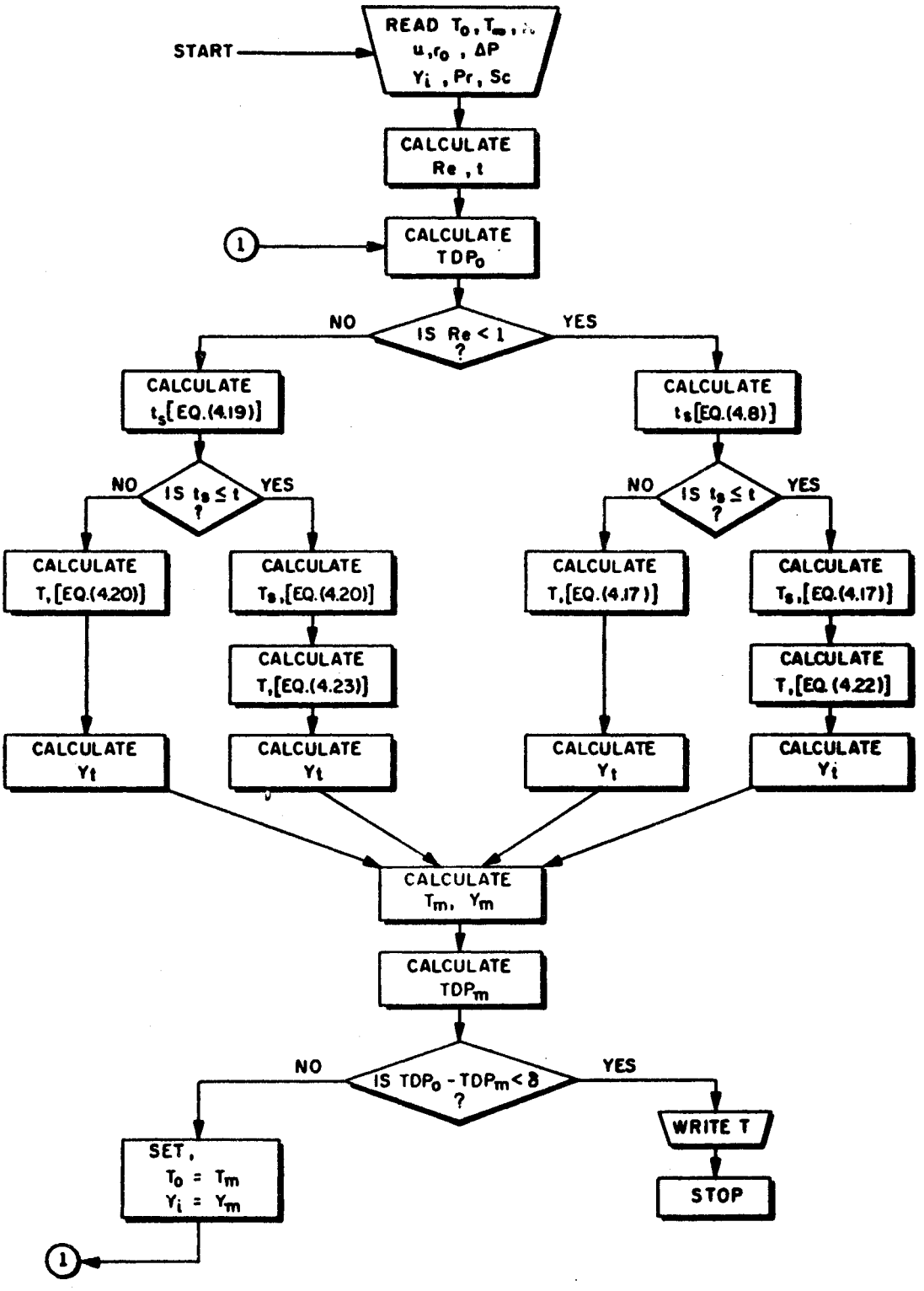

Figure 3. Computer Flow Chart

CHAPTER VI

RESULTS

Two types of cooling fluid were considered, fresh water and brine (NaCl solutions). Some performance data has been published on spray cooling systems using fresh water [3]. The model was first solved for fresh water, simulating the conditions for which this performance data was available. Values were assumed for R/r_o and relative humidity which yielded the closest fit to the published data. A parametric analysis was then performed to establish curves that could be used for determining the effect of various parameters on the performance of spray cooling system.

Next, the effect of NaCl concentration on spray cooling was determined by introducing specific heat, latent heat of vaporization, specific volume, and vapor pressure data for brine solutions into the mathematical model. Again a parametric analysis was performed to establish curves for design work.

6.1 Fresh Water Results

Only the wet bulb temperature was included in the published data on spray pond performance. This value was 70°F [3]. Various relative humidities (and thus dry bulb temperatures) were assumed, using a wet bulb temperature of 70°F and keeping the ratio R/r_o constant, until there was a minimum difference in the slope between the predicted and

actual performance curves as shown in Figure 4. The humidity so selected was 0.78. The corresponding dry bulb temperature was 75° F.

Since there was no data available to determine the best value of the ratio R/r_o, calculations were performed for different values of this ratio to determine the value that best fits the published data. This value was found to be 18.

Figure 5 shows a comparison of calculated spray pond performance to published data for a 0.78 relative humidity and a value of 18 for the ratio R/r_o.

Figure 6 shows the effect of wet bulb temperature on the cooling pond performance when compared to published data. The cooling effect (the temperature decrease due to spraying water or brine) increases as the wet bulb temperature decreases. The wet bulb temperature represents the lowest temperature than can be achieved by evaporation cooling.

Figure 7 shows the spray pond temperature at the saturation time and at the total exposure time for different values of entering temperature, T_o. Table I gives the corresponding published data at 70° F wet bulb temperature. These results compare quite favorably, the greatest deviation being 6.5%. This slight deviation is possibly due to the assumption that the cooling and evaporation process were assumed to be stationary. Also, the assumption that the droplets have uniform temperature would yield a conservative estimate.

The effects of the droplet diameter and wind velocity on spray pond performance are shown in Figures 8 and 9 and Table II. As can be readily seen, the cooling effect increases as the droplet diameter decreases which is to be expected because of the increase in the ratio of cooling surface area to the volume. The percentage change in the cooling effect

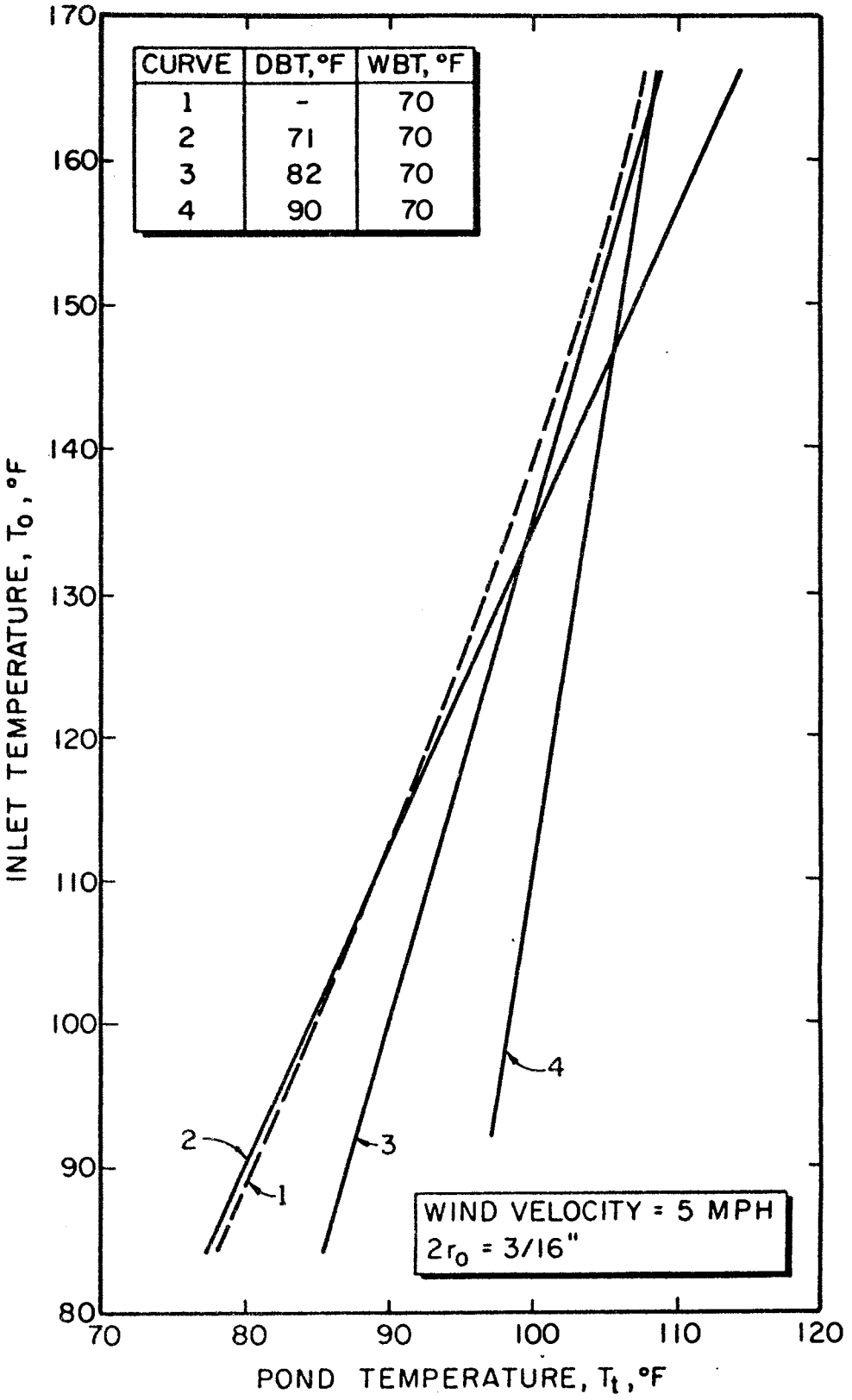

Figure 4. Comparison of Spray Pond Performance Curve

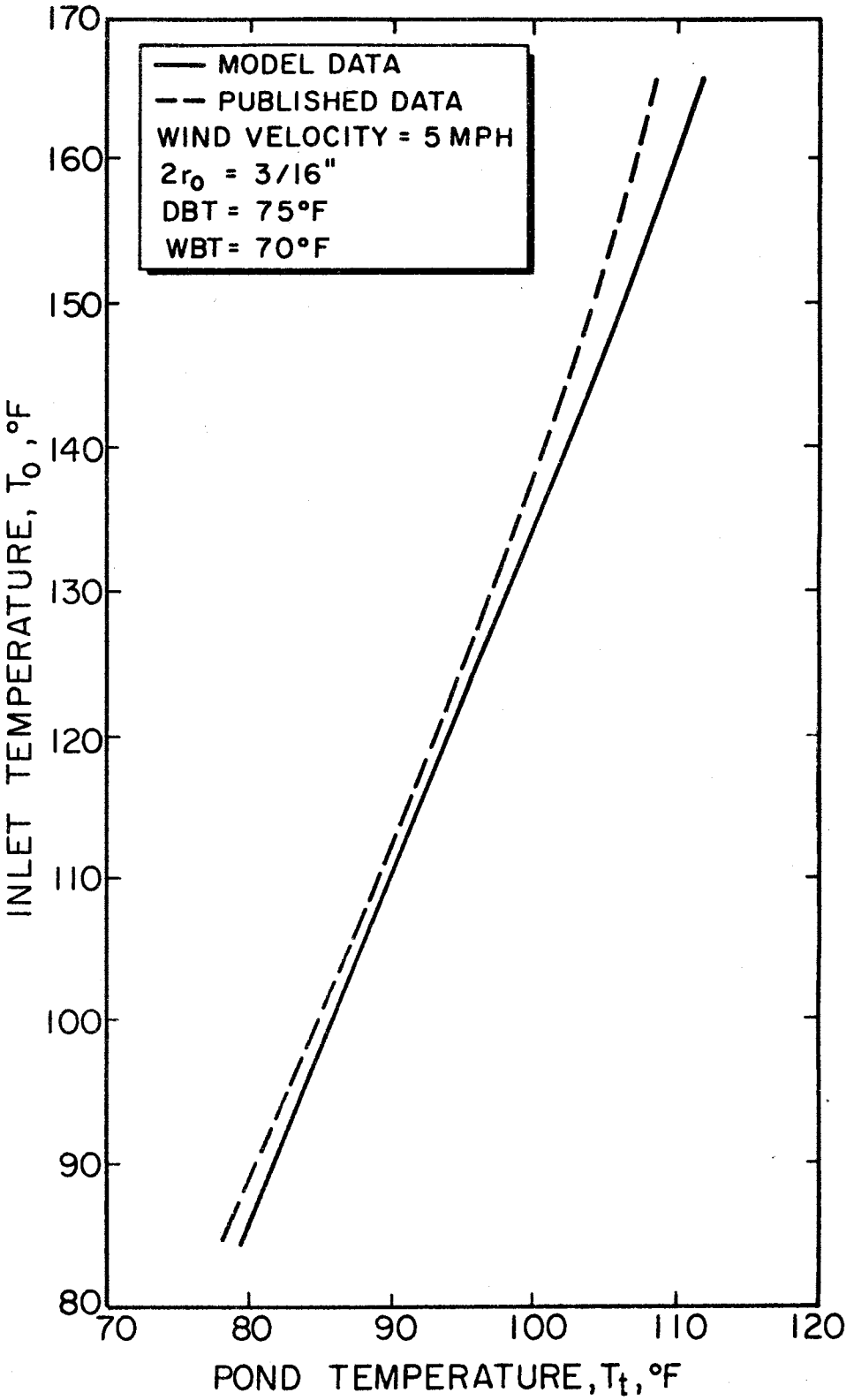

Figure 5. Comparison of Spray Pond Performance Curve (WBT = 70° F)

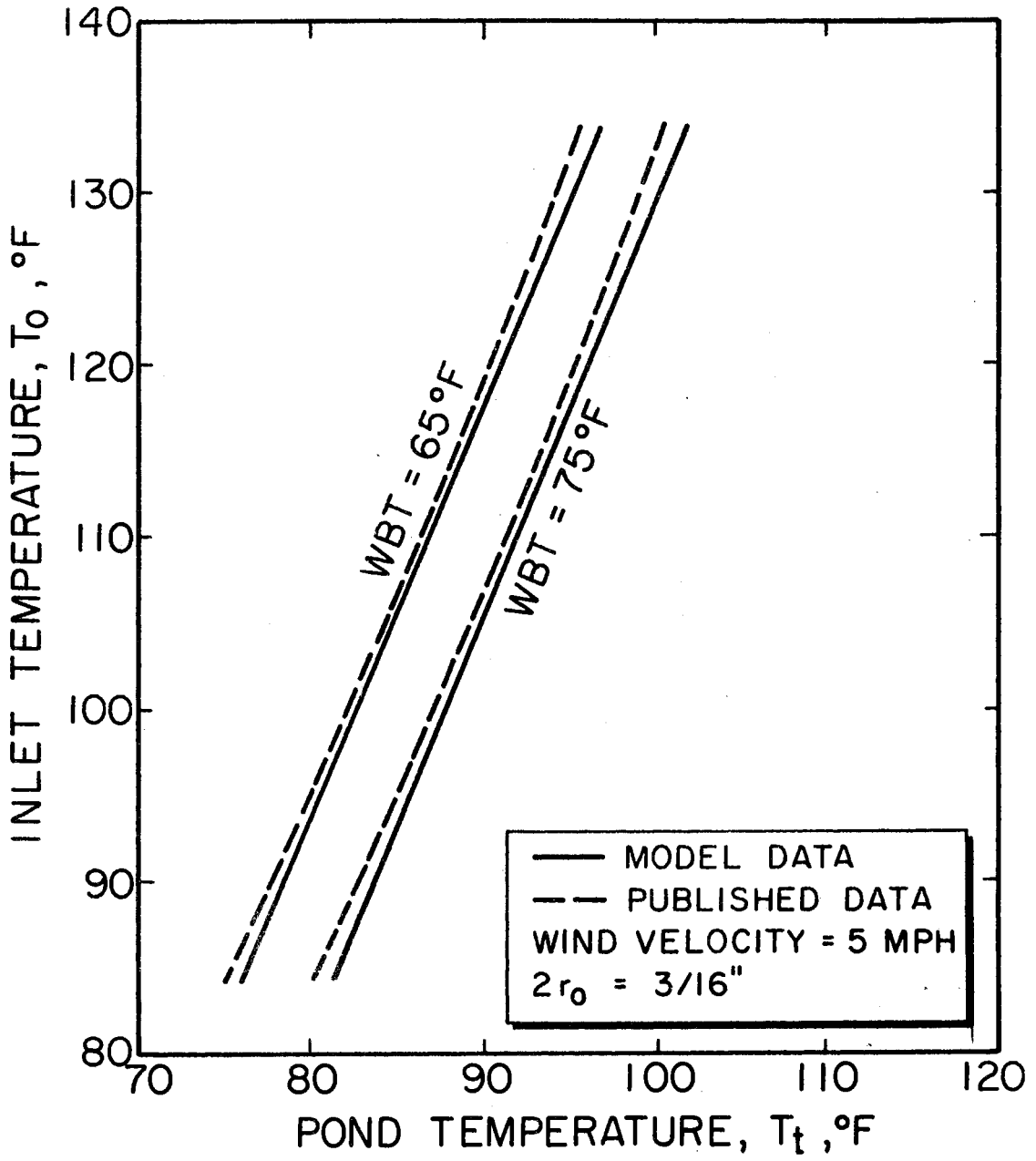

Figure 6. The Effect of Wet Bulb Temperature on Spray Pond Performance Curves

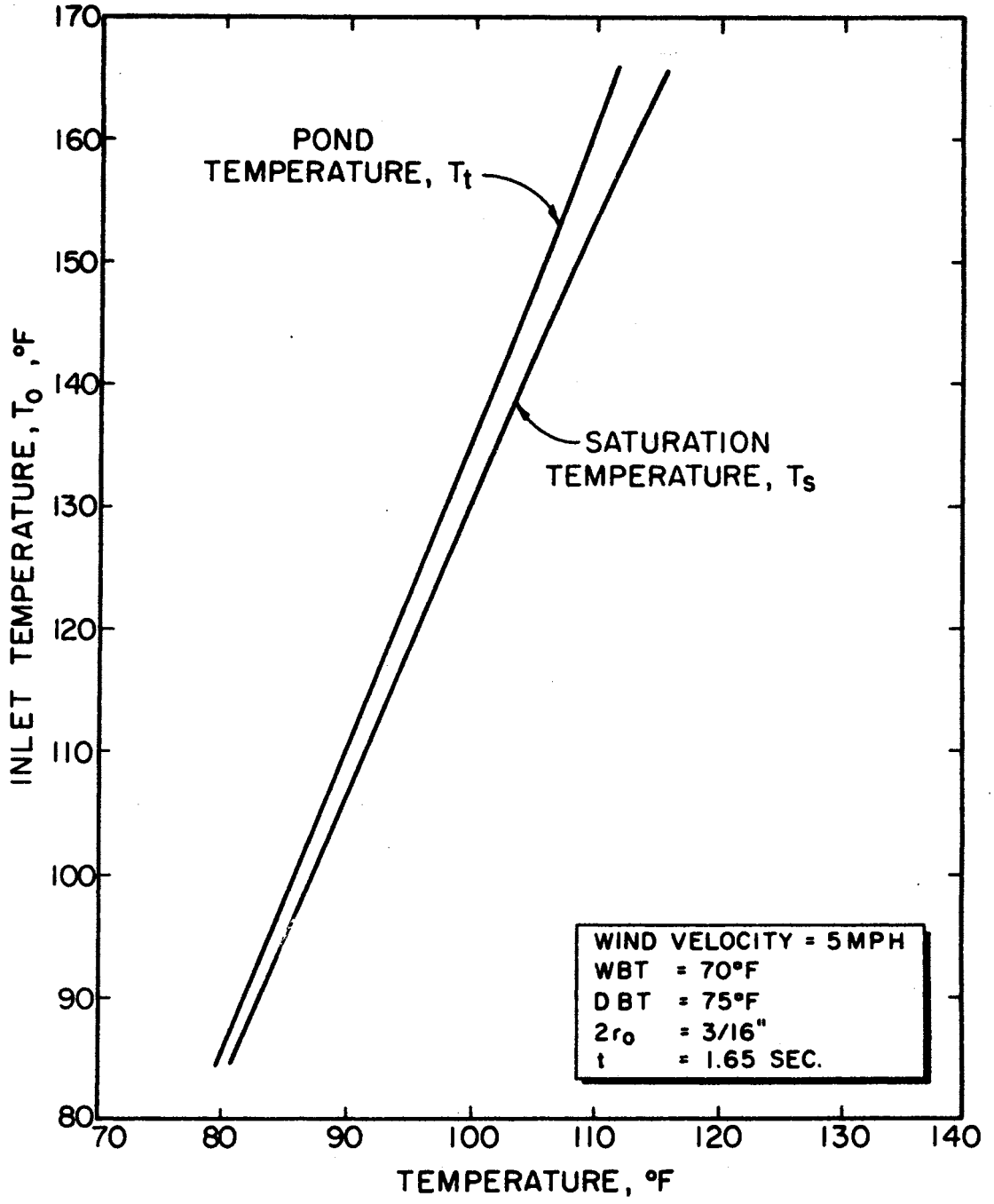

Figure 7. Spray Pond Model Data at Saturation and Total Exposure Time

TABLE I

SPRAY POND MODEL DATA AT SATURATION AND TOTAL EXPOSURE TIME
(Wet Bulb Temperature = 70°F; Dry Bulb Temperature = 75°F;
Droplet Diameter = 3/16"; Wind Velocity = 5 m.p.h.;
Total Exposure Time = 1.65 sec.)

T_o, °F	T_t, °F Published Data	Model Data		
		t_s, second	T_s, °F	T_t, °F
85	78.4	1.446710	80.8	79.7
90	80.5	1.435970	83.3	81.8
95	82.5	1.426375	85.4	83.8
100	85.0	1.424902	87.3	85.8
105	87.0	1.414145	89.4	87.8
110	89.0	1.401707	91.8	89.8
115	91.0	1.393661	93.6	91.8
120	93.0	1.383070	95.7	93.8
125	95.0	1.377562	97.7	95.8
130	97.0	1.355964	100.0	97.7
135	99.0	1.350490	102.1	99.7
140	100.7	1.344508	104.7	101.7
145	102.0	1.329150	106.6	103.7
150	104.0	1.337515	108.4	105.7
155	105.0	1.326480	110.7	107.6
160	106.5	1.307940	113.1	109.5

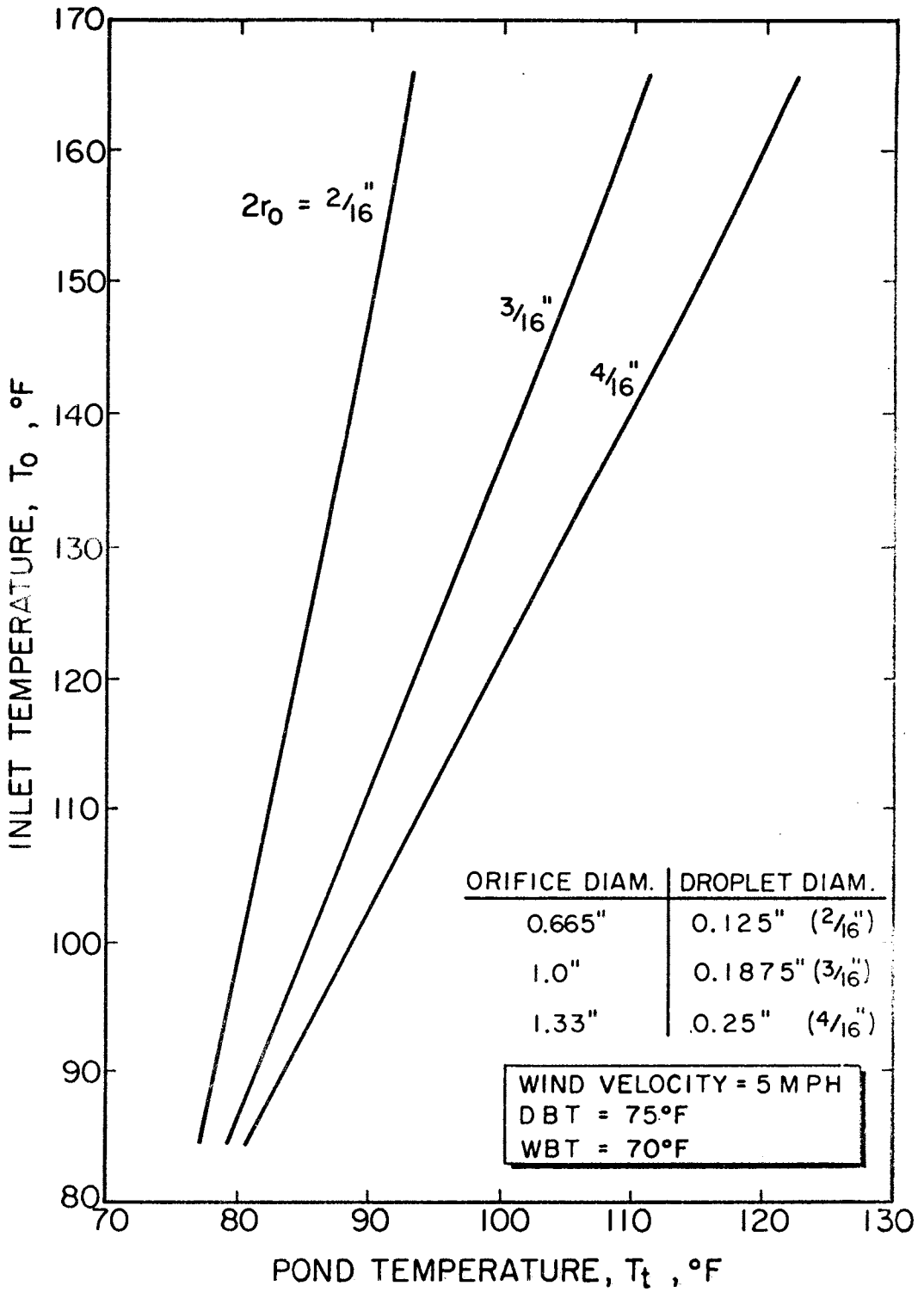

Figure 8. Spray Pond Performance Curves for Different Droplet Diameters

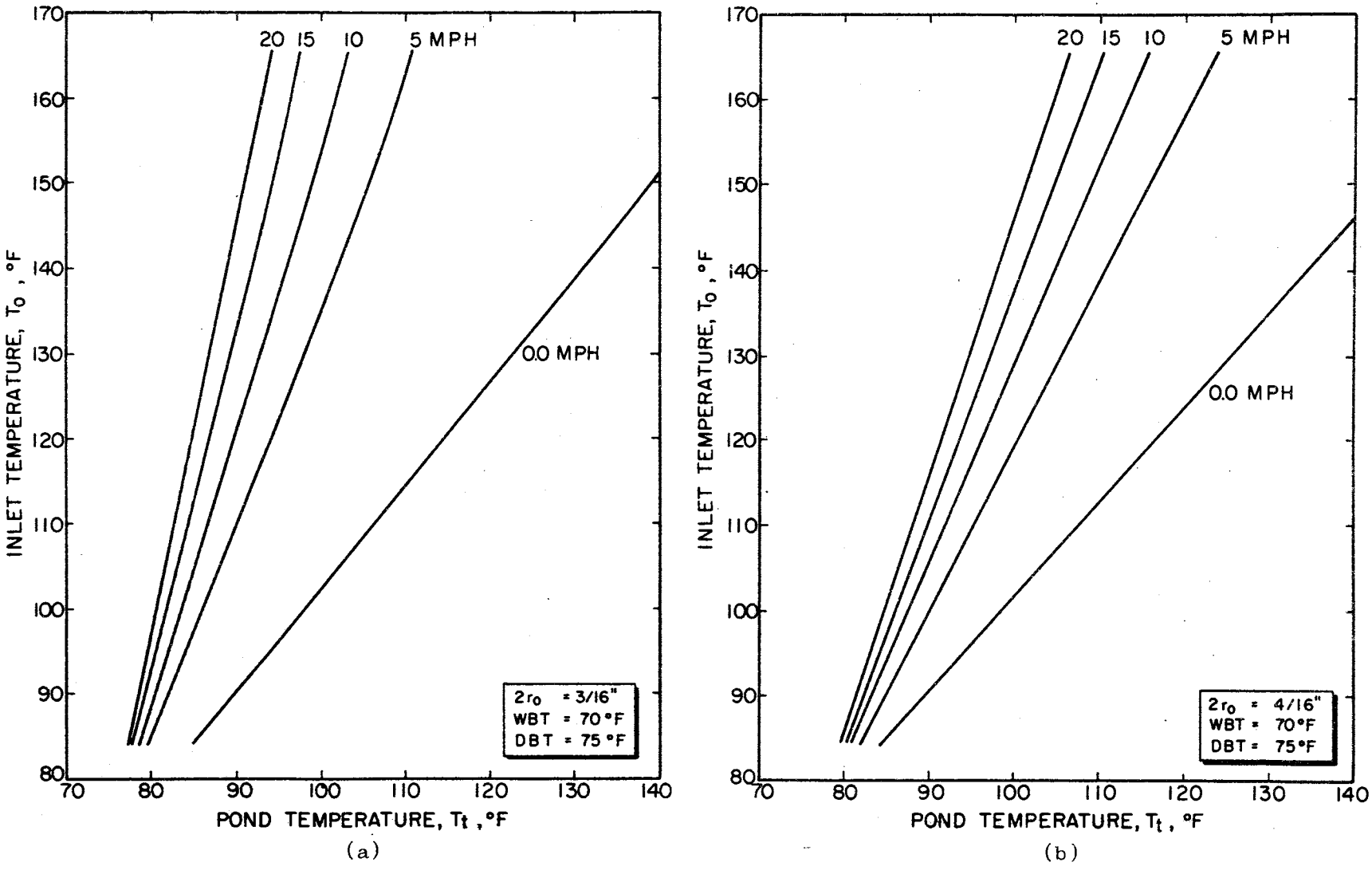

Figure 9. Spray Pond Performance Curves for Various Wind Velocities

TABLE II

SPRAY POND MODEL DATA FOR VARIOUS WIND VELOCITIES
(Wet Bulb Temperature = 70°F;
Dry Bulb Temperature = 75°F;
Droplet Diameter = 2/16")

T_o, °F	T_t, °F				
	0.0 m.p.h.	5 m.p.h.	10 m.p.h.	15 m.p.h.	20 m.p.h.
85	83.4	77.5	76.5	76.0	75.7
90	86.9	78.5	77.1	76.4	76.0
95	90.4	79.5	77.7	76.8	76.3
100	93.8	80.5	78.3	77.2	76.6
105	97.3	81.5	78.9	77.6	76.9
110	100.2	82.5	79.5	78.1	77.2
115	104.2	83.5	80.1	78.5	77.5
120	107.7	84.5	80.7	78.9	77.8
125	111.1	85.5	81.3	79.3	78.1
130	114.6	86.5	81.9	79.7	78.3
135	118.2	87.5	82.5	80.1	78.6
140	121.7	88.6	83.1	80.5	78.9
145	125.0	89.5	83.7	80.9	79.2
150	128.5	90.5	84.3	81.2	79.5
155	132.0	91.5	84.9	81.4	79.8
160	135.5	92.5	85.4	81.9	80.0
165	139.0	93.0	86.0	82.2	80.2

for a reduction in droplet diameters from 3/16" to 2/16" is from 43% of a 160° F water inlet temperature where,

$$43\% = 100 \times \frac{\text{Cooling range for 2/16" droplet} - \text{Cooling range for 3/16" droplet}}{\text{Cooling range for 3/16" droplet}},$$

to 27% at a 90° F water inlet temperature. These results were predicted for a wet bulb temperature of 70° F and dry bulb temperature 75° F. An increase in cooling effect also occurred as the wind velocity increased due to increased air circulation around the spray droplets. The percentage change in cooling effect for an increase in wind velocity from 5 m.p.h. to 20 m.p.h. is from 41% for a 140° F water inlet temperature to 31% for a 90° F water inlet temperature. These results were predicted for a wet bulb temperature of 70° F and dry bulb temperature of 75° F.

If it is necessary to cool water through a larger temperature range, the spray pond could be staged. With this method the water is initially sprayed, collected, and then resprayed in another part of a sectionalized pond basin. Figure 10 shows the cooling effect of three stages. The percentage change in the cooling effect obtained from the second stage is from 50% for a 160° F water inlet temperature to 26% for a 90° F water inlet temperature.

6.2 Salt Water Results

Having established optimum values for R/r_o and relative humidity for fresh water using published data, salt water then was analyzed. Calculations were performed using thermodynamic properties of salt water. Figure 11 and Table III show the spray pond performance of salt water for different salt concentrations. The cooling effect increases as the salt percentage increases. This is due to the fact that the

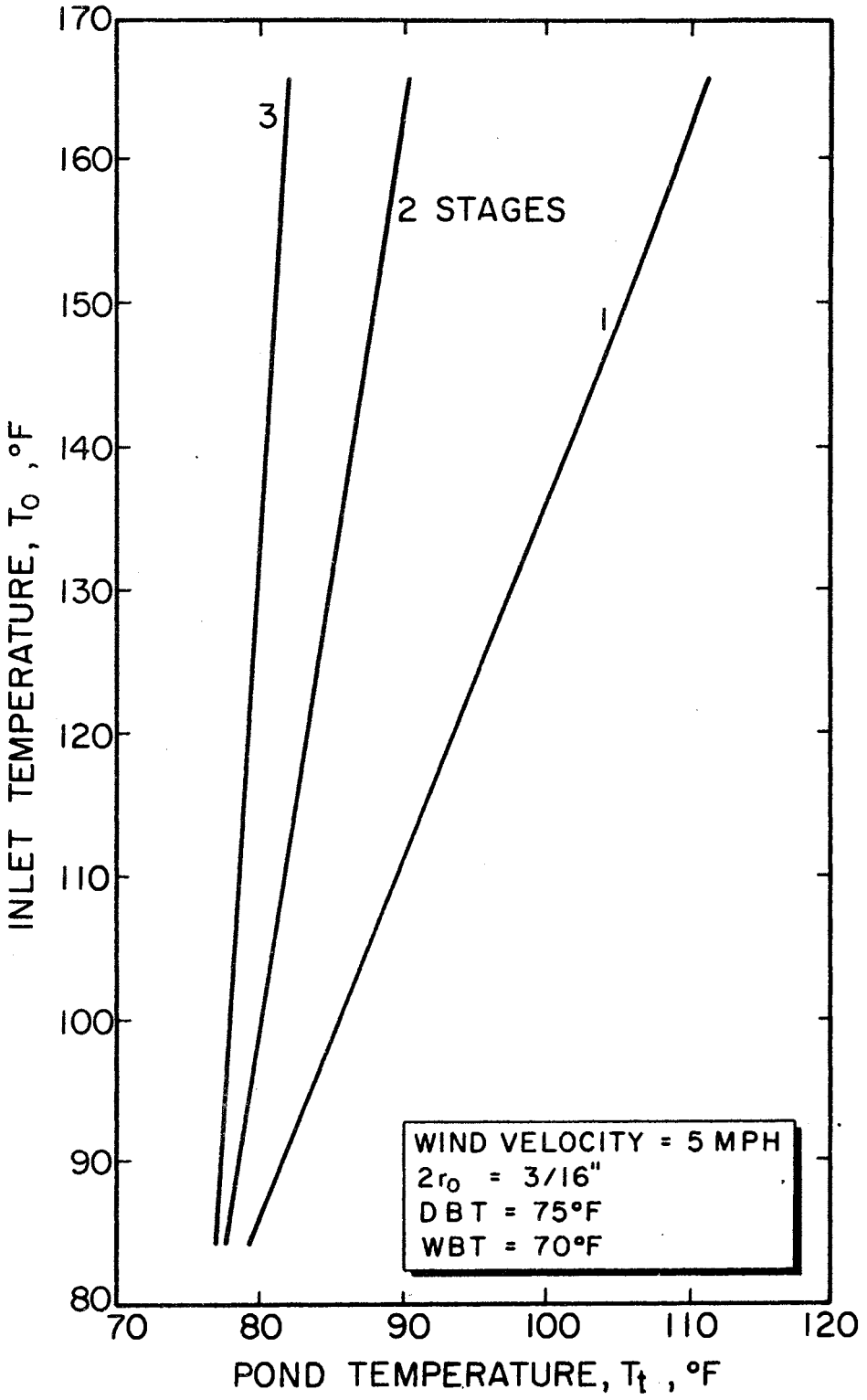

Figure 10. Spray Pond Performance Curves with Staging

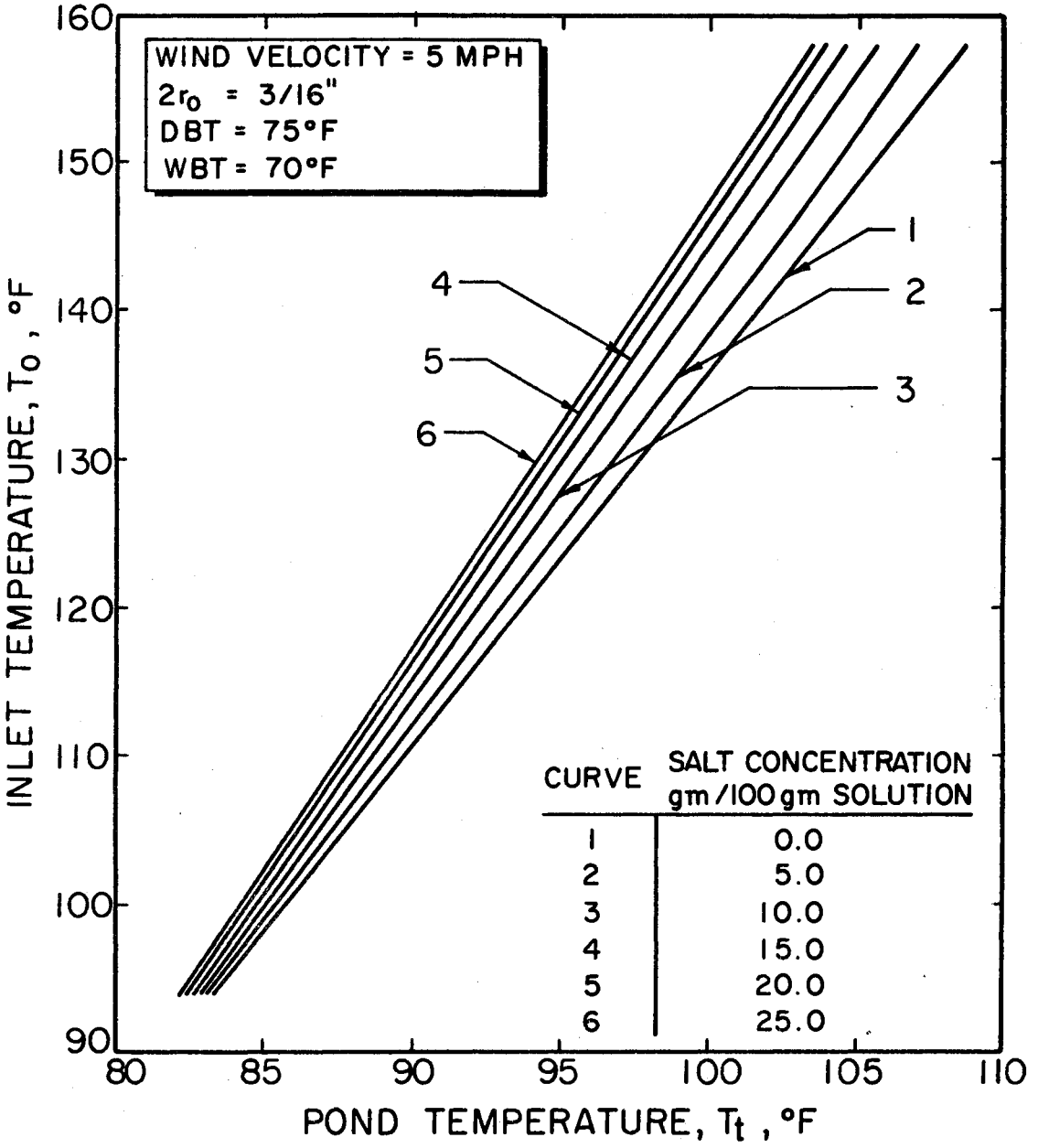

Figure 11. Spray Pond Model Data for Brine at Varying Salt Concentration

TABLE III

SPRAY POND MODEL DATA FOR BRINE AT VARYING SALT CONCENTRATION
(Wet Bulb Temperature = 70°F; Dry Bulb Temperature = 75°F;
Droplet Diameter = 3/16"; Wind Velocity = 5 m.p.h.;
Salt Concentration in gm/100 gm Solution)

T_o, °F	T_t, °F					
	0.0 gm/100 gm	5 gm/100 gm	10 gm/100 gm	15 gm/100 gm	20 gm/100 gm	25 gm/100 gm
85	79.9	79.7	79.5	79.4	79.3	79.2
90	81.8	81.6	81.4	81.2	81.0	80.9
95	83.8	83.5	83.2	82.9	82.7	82.6
100	85.8	85.4	85.0	84.7	84.4	84.3
105	87.8	87.3	86.5	86.4	86.2	86.0
110	89.8	89.2	88.7	88.2	87.2	87.7
115	91.8	91.1	90.5	90.0	89.6	89.4
120	93.8	93.1	92.3	91.7	91.3	91.1
125	95.8	95.0	94.2	93.5	92.9	92.7
130	97.7	96.8	95.9	95.2	94.6	94.4
135	99.7	98.7	97.8	96.2	96.3	96.1
140	101.7	100.7	99.6	98.7	98.1	97.7
145	103.7	102.5	101.4	100.4	97.7	99.4
150	105.7	104.4	103.3	102.2	101.4	101.0
155	107.6	106.3	105.2	103.9	103.0	102.7
160	109.5	108.3	106.8	105.6	104.7	104.3

specific heat of NaCl solutions decreases as the percentage of salt concentration increases [14].

Figure 12 shows a comparison between fresh water and simulated normal sea water which has a salt concentration of 3.4483 gm/100 gm solution [15].

Figure 13 and Table IV show the spray pond model data for various stages using salt water of different salt concentration. The effect of staging was the same as for the fresh water case. The effects of droplet diameters and wind velocity on the spray pond performance of salt water of different salt concentration are shown in Figures 14 through 16 and Tables V through XIV. These results show changes in temperature as functions of droplet diameter and wind velocity which are similar to the fresh water case.

Table XV shows that the water loss due to evaporation is very small. The loss is slightly less for brine. This slight variation is due to the effect of salt concentration on the vapor concentration gradient in case of brine. The vapor concentration gradient decreases as the percentage of salt concentration increases.

It was noticed that the effect of variation in wind velocity was only on the rate of evaporation. Since the evaporation stops when the cell becomes saturated with water vapor, the variation in wind velocity has no effect on the evaporation quantity.

Table XVI shows a comparison of calculated results to results obtained from the Spraying System Company. The model results were in very close agreement with their reported results for different values of wet bulb and dry bulb temperatures.

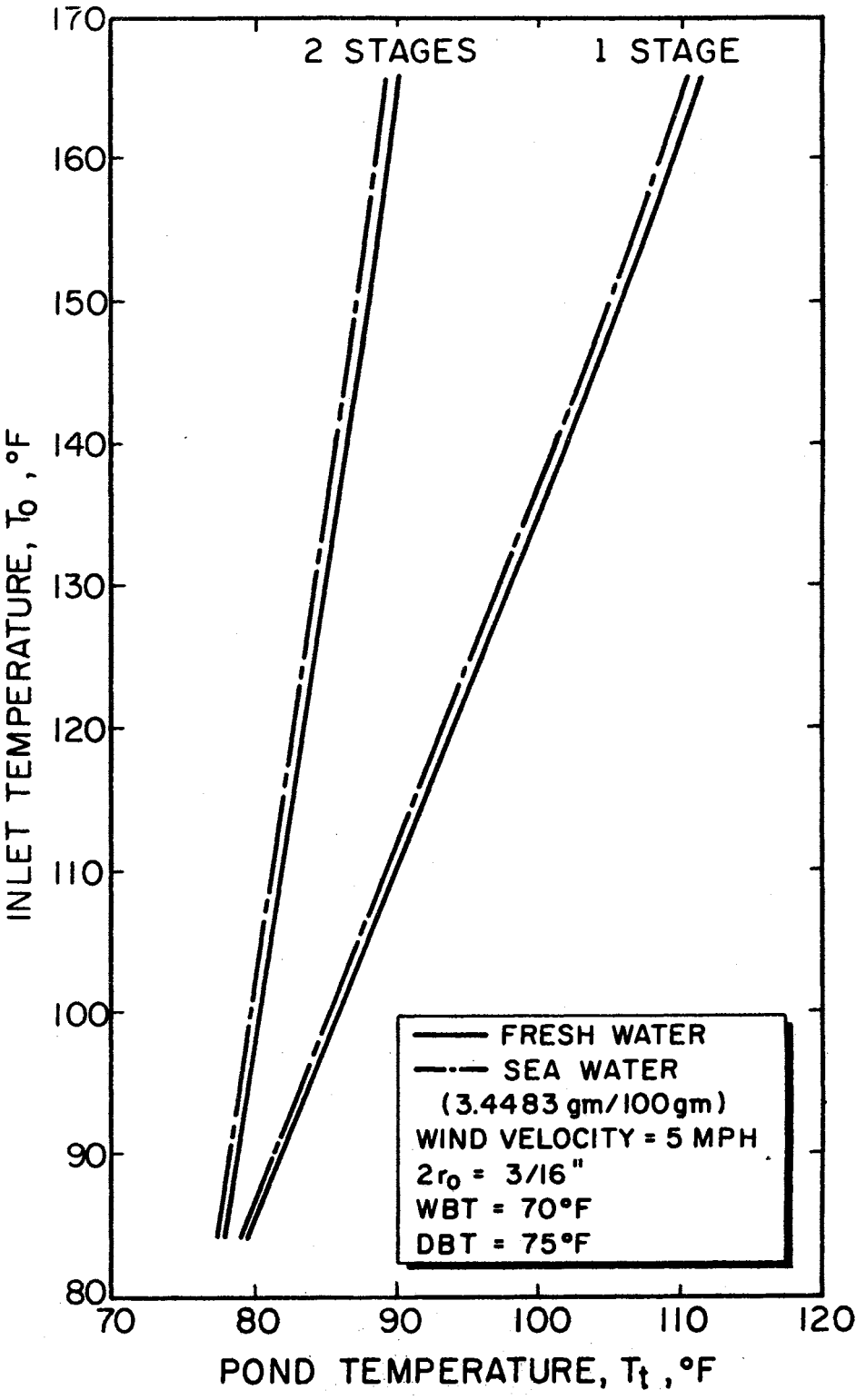

Figure 12. Spray Pond Model for Fresh Water and Sea Water

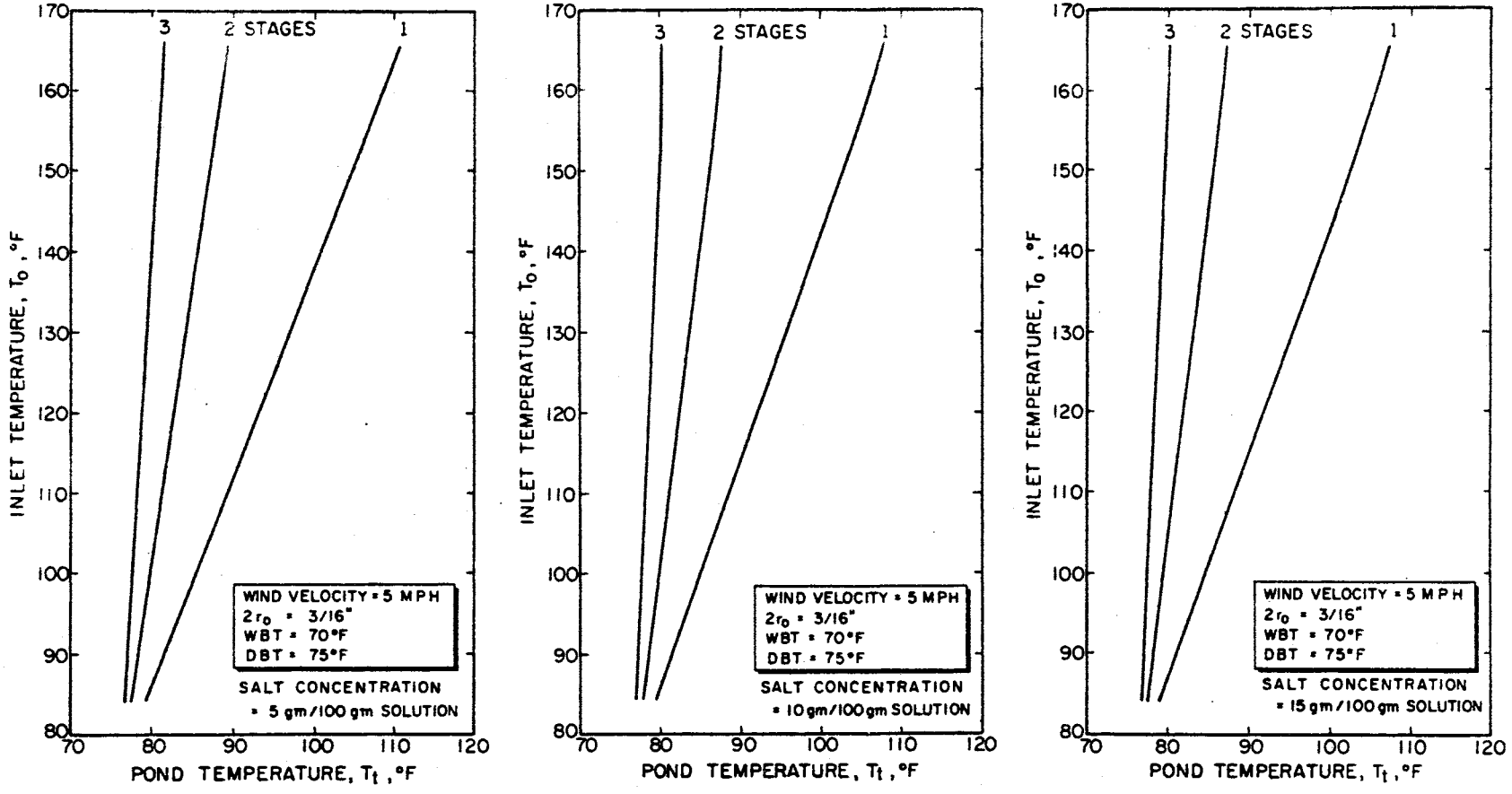

Figure 13. Brine Spray Pond Performance Curves with Staging

TABLE IV

BRINE SPRAY POND MODEL DATA WITH STAGING
(Wet Bulb Temperature = 70°F;
Dry Bulb Temperature = 75°F;
Droplet Diameter = 3/16";
Wind Velocity = 5 m.p.h.)

(A) Salt Concentration = 20 gm/100 gm Solution				(B) Salt Concentration = 25 gm/100 gm Solution			
T_o, °F	T_t, °F			T_o, °F	T_t, °F		
	1 Stage	2 Stages	3 Stages		1 Stage	2 Stages	3 Stages
85	79.3	77.3	76.6	85	79.2	77.3	76.6
90	81.0	77.9	76.9	90	80.9	77.9	76.8
95	82.7	78.5	77.1	95	82.6	78.4	77.0
100	84.4	79.1	77.3	100	84.3	79.0	77.2
105	86.2	79.7	77.5	105	86.0	79.6	77.4
110	87.2	80.3	77.7	110	87.7	80.1	77.6
115	89.6	80.9	77.9	115	89.4	80.7	77.8
120	91.3	81.4	78.1	120	91.1	81.3	78.0
125	92.9	82.0	78.3	125	92.7	81.8	78.2
130	94.6	82.6	78.5	130	94.4	82.4	78.4
135	96.3	83.2	78.7	135	96.1	83.0	78.5
140	98.1	83.8	78.9	140	97.7	83.5	78.7
145	99.7	84.3	79.1	145	99.4	84.1	78.9
150	101.4	84.9	79.3	150	101.0	84.7	79.1
155	103.0	85.5	79.5	155	102.7	85.2	79.3
160	104.7	86.0	79.7	160	104.3	85.8	79.5
165	106.4	87.1	79.9	165	106.1	86.6	79.7

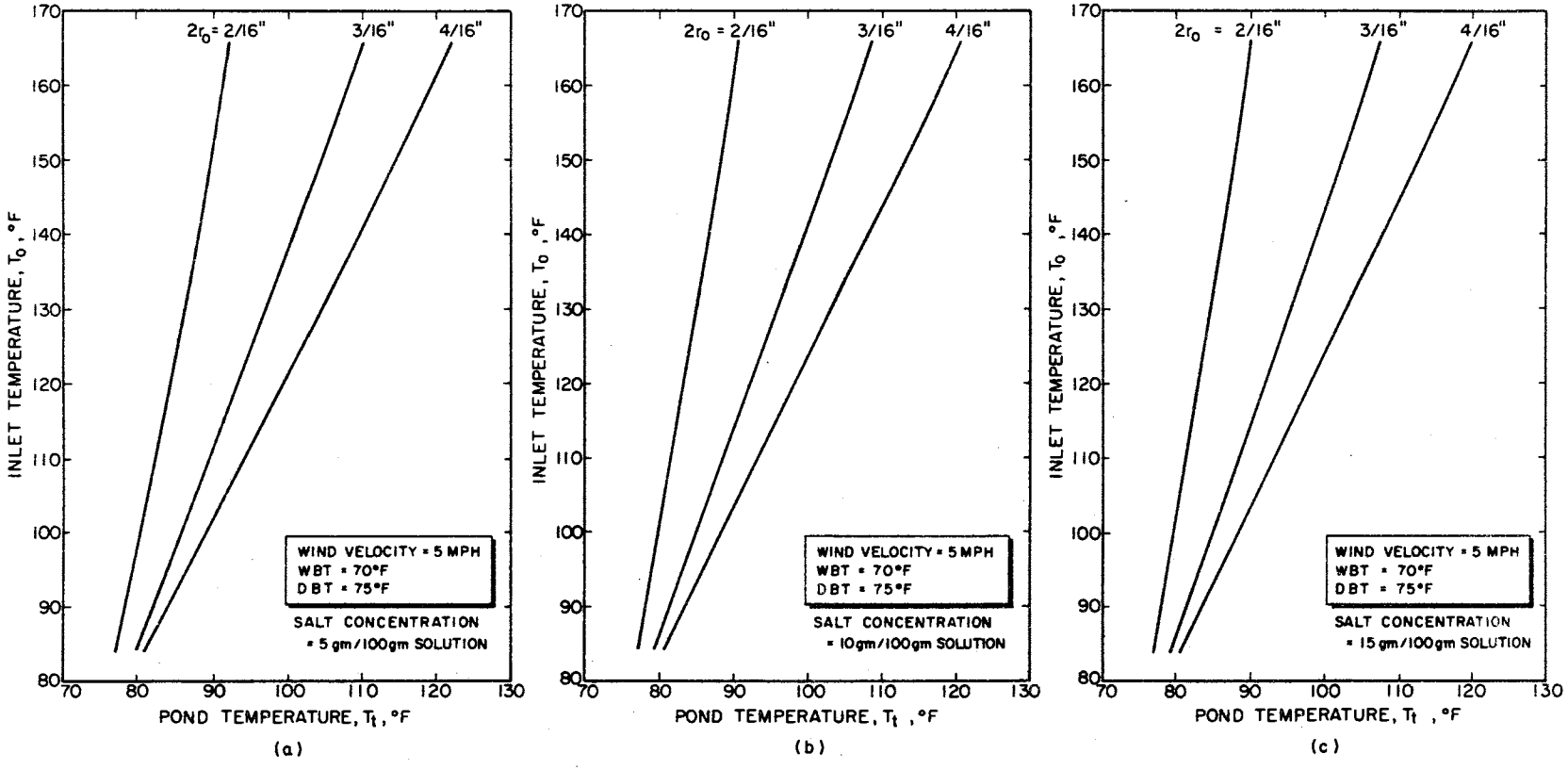

Figure 14. Brine Spray Pond Performance Curves for Different Droplet Diameters

TABLE V

BRINE SPRAY POND MODEL DATA FOR DIFFERENT DROPLET DIAMETERS
(Wet Bulb Temperature = 70°F; Dry Bulb Temperature = 75°F;
Wind Velocity = 5 m.p.h.)

(A) Salt Concentration = 20 gm/100 gm Solution				(B) Salt Concentration = 25 gm/100 gm Solution			
T_o, °F	T_t, °F			T_o, °F	T_t, °F		
	$2r_o$ = 2/16"	$2r_o$ = 3/16"	$2r_o$ = 4/16"		$2r_o$ = 2/16"	$2r_o$ = 3/16"	$2r_o$ = 4/16"
85	76.9	79.3	80.9	85	76.9	79.2	80.9
90	77.7	81.0	83.3	90	77.6	80.9	83.2
95	78.5	82.7	85.7	95	78.4	82.6	85.6
100	79.3	84.4	88.0	100	79.2	84.3	87.9
105	80.0	86.2	90.4	105	79.7	86.0	90.3
110	80.8	87.2	92.8	110	80.7	87.7	92.6
115	81.6	89.6	95.1	115	81.4	89.4	95.0
120	82.3	91.3	97.5	120	82.2	91.1	97.3
125	83.1	92.9	99.8	125	82.9	92.7	99.6
130	83.8	94.6	102.2	130	83.6	94.4	102.0
135	84.6	96.3	104.5	135	84.3	96.1	104.3
140	85.3	98.1	106.9	140	85.1	97.7	106.6
145	86.1	99.7	109.3	145	85.8	99.4	108.9
150	86.9	101.4	111.6	150	86.5	101.0	111.3
155	87.5	103.0	114.0	155	87.2	102.7	113.6
160	88.3	104.7	116.3	160	87.9	104.3	115.9
165	89.0	106.6	118.8	165	88.8	105.5	118.0

TABLE VI

BRINE SPRAY POND MODEL DATA FOR VARIOUS WIND VELOCITIES
(Wet Bulb Temperature = 70°F; Dry Bulb Temperature = 75°F;
Droplet Diameter = 2/16"; Salt
Concentration = 5 gm/100gm)

T_o, °F	T_t, °F				
	0.0 m.p.h.	5 m.p.h.	10 m.p.h.	15 m.p.h.	20 m.p.h.
85	83.4	77.3	76.4	75.9	75.6
90	86.8	78.3	76.9	76.3	75.9
95	90.2	79.2	77.4	76.6	76.2
100	93.6	80.1	78.0	77.0	76.4
105	97.0	81.1	78.5	77.4	76.7
110	100.4	82.0	79.1	77.7	76.9
115	103.8	82.9	79.6	78.1	77.2
120	107.3	83.9	80.2	78.4	77.4
125	110.7	84.8	80.7	78.8	77.7
130	114.2	85.7	81.2	79.1	77.9
135	117.6	86.6	81.8	79.5	78.2
140	121.0	87.5	82.3	79.8	78.4
145	124.5	88.5	82.9	80.2	78.7
150	127.9	89.4	83.4	80.6	78.9
155	131.5	90.3	83.9	80.9	79.2
160	134.7	91.2	84.4	81.2	79.4
165	137.5	92.0	85.0	81.8	79.5

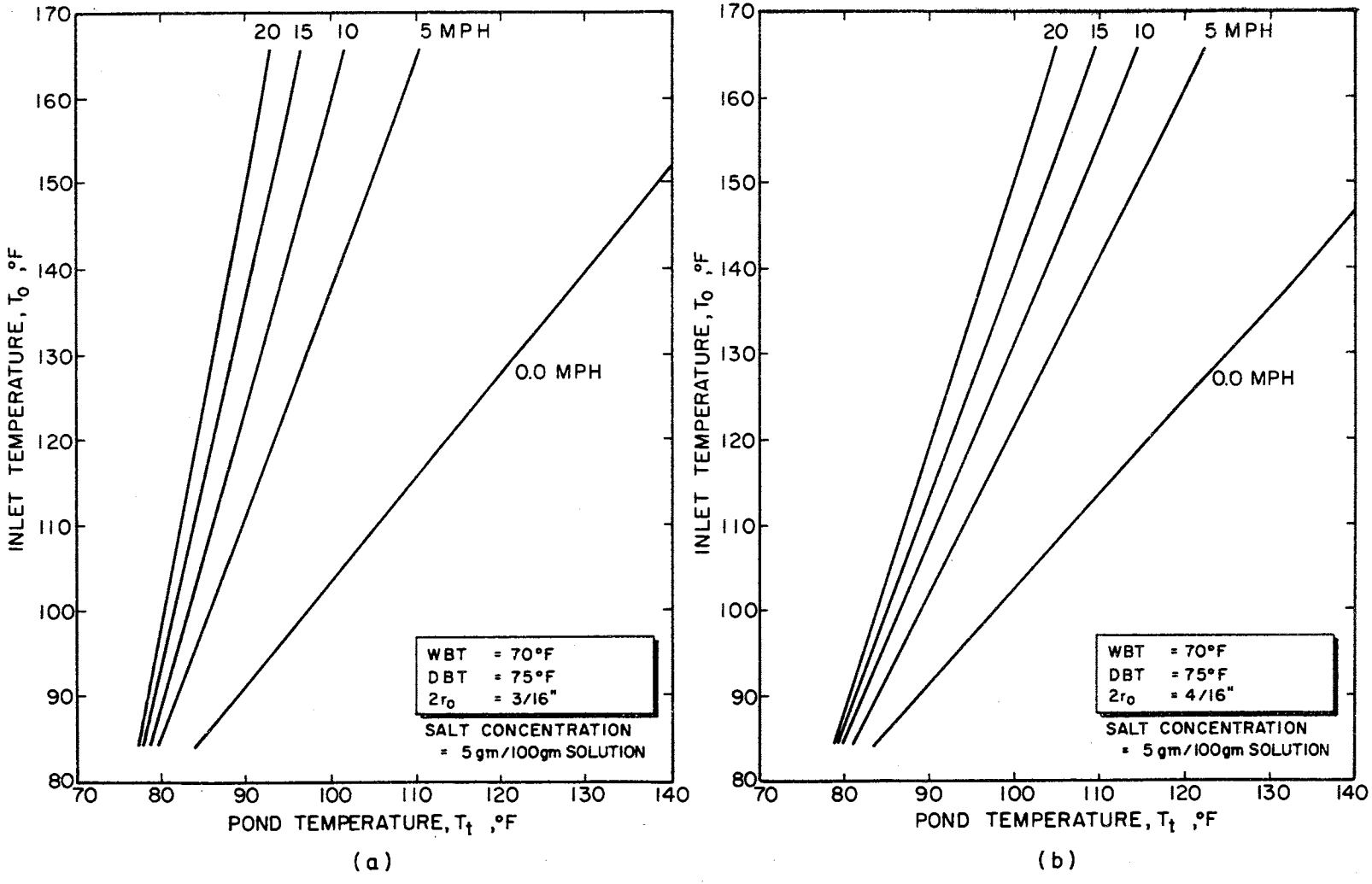

Figure 15. Brine Spray Pond Performance Curves for Various Wind Velocities (Salt Concentration = 5 gm/100 gm)

TABLE VII

BRINE SPRAY POND MODEL DATA FOR VARIOUS WIND VELOCITIES
(Wet Bulb Temperature = 70°F; Dry Bulb Temperature = 75°F;
Droplet Diameter = 2/16"; Salt
Concentration = 10 gm/100 gm)

T_o, °F	T_t, °F				
	0.0 m.p.h.	5 m.p.h.	10 m.p.h.	15 m.p.h.	20 m.p.h.
85	83.3	77.2	76.2	75.8	75.6
90	86.6	78.0	76.7	76.1	75.8
95	90.0	78.9	77.2	76.5	76.0
100	93.4	79.8	77.7	76.8	76.2
105	96.8	80.6	78.2	77.1	76.5
110	100.1	81.5	78.7	77.4	76.7
115	103.5	82.4	79.2	77.7	76.9
120	106.9	83.2	79.7	78.1	77.1
125	110.2	84.1	80.2	78.4	77.3
130	113.6	84.9	80.7	78.7	77.6
135	117.0	85.8	81.2	79.0	77.8
140	120.3	86.6	81.6	79.3	78.0
145	123.8	87.5	82.1	79.6	78.2
150	127.3	88.4	82.6	79.9	78.4
155	130.5	89.1	83.0	80.2	78.6
160	133.9	90.0	83.5	80.5	78.8
165	137.0	90.8	84.0	81.0	79.2

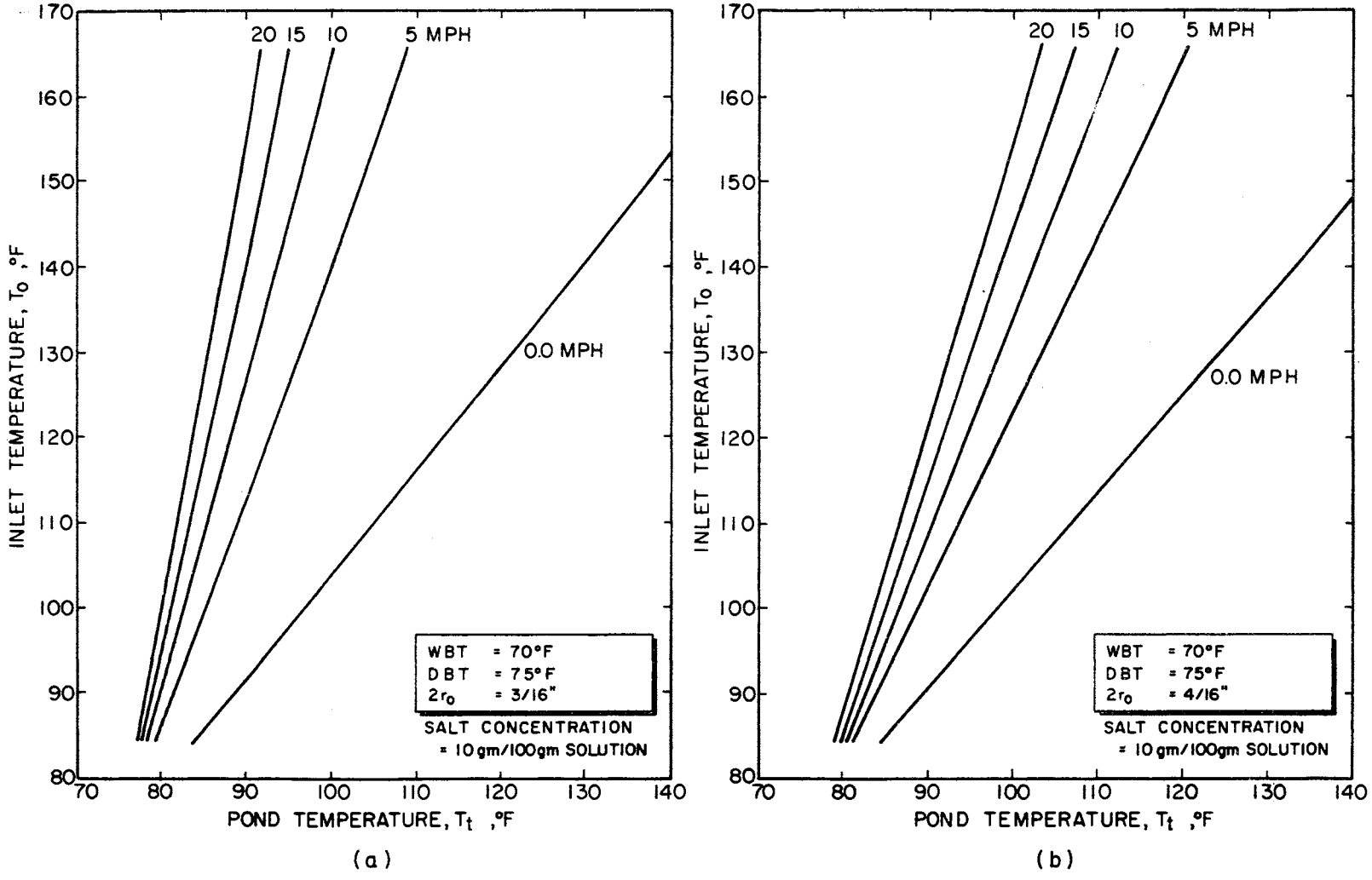

Figure 16. Brine Spray Pond Performance Curves for Various Wind Velocities (Salt Concentration = 10 gm/100 gm)

TABLE VIII

BRINE SPRAY POND MODEL DATA FOR VARIOUS WIND VELOCITIES
(Wet Bulb Temperature = 70°F; Dry Bulb Temperature = 75°F;
Droplet Diameter = 2/16"; Salt
Concentration = 15 gm/100 gm)

T_o, °F	T_t, °F				
	0.0 m.p.h.	5 m.p.h.	10 m.p.h.	15 m.p.h.	20 m.p.h.
85	83.2	77.0	76.1	75.7	75.5
90	86.5	77.9	76.6	76.0	75.7
95	89.9	78.7	77.0	76.3	75.9
100	93.2	79.5	77.5	76.6	76.1
105	96.5	80.4	78.0	76.9	76.3
110	99.8	81.1	78.4	77.2	76.5
115	103.1	81.9	78.8	77.5	76.7
120	106.5	82.7	79.3	77.8	76.9
125	109.8	83.5	79.7	78.0	77.0
130	113.2	84.3	80.2	78.3	77.3
135	116.4	85.1	80.6	78.6	77.4
140	119.8	85.9	81.1	78.9	77.7
145	123.1	86.6	81.5	79.1	77.8
150	126.4	87.5	81.9	79.4	78.0
155	129.8	88.2	82.3	79.7	78.2
160	133.1	89.0	82.8	79.9	78.4

TABLE IX

BRINE SPRAY POND MODEL DATA FOR VARIOUS WIND VELOCITIES
(Wet Bulb Temperature = 70°F; Dry Bulb Temperature = 75°F;
Droplet Diameter = 3/16"; Salt
Concentration = 15 gm/100 gm)

T_o, °F	T_t, °F				
	0.0 m.p.h.	5 m.p.h.	10 m.p.h.	15 m.p.h.	20 m.p.h.
85	84.1	79.4	78.2	77.5	77.1
90	88.4	81.2	79.5	78.5	77.9
95	92.4	82.9	80.8	79.5	78.7
100	96.5	84.7	82.1	80.6	79.5
105	100.7	86.4	83.3	81.5	80.3
110	104.8	88.2	84.6	82.6	81.2
115	109.9	90.0	85.9	83.6	82.0
120	113.0	91.7	87.2	84.5	82.8
125	117.1	93.5	88.5	85.6	83.6
130	121.2	95.2	89.7	86.5	84.4
135	125.2	96.2	90.9	87.5	85.2
140	129.3	98.7	92.2	88.5	86.0
145	133.4	100.4	93.5	89.5	86.8
150	137.4	102.2	94.7	90.4	87.5
155	141.5	103.9	96.0	91.4	88.4
160	145.5	105.6	97.2	92.4	89.1

TABLE X

BRINE SPRAY POND MODEL DATA FOR VARIOUS WIND VELOCITIES
(Wet Bulb Temperature = 70°F; Dry Bulb Temperature = 75°F;
Droplet Diameter = 4/16"; Salt
Concentration = 15 gm/100 gm)

T_o, °F	T_t, °F				
	0.0 m.p.h.	5 m.p.h.	10 m.p.h.	15 m.p.h.	20 m.p.h.
85	84.5	81.0	79.9	79.2	78.7
90	89.0	83.4	81.9	80.9	80.1
95	93.5	85.8	83.8	82.5	81.6
100	98.0	88.2	85.8	84.2	83.1
105	102.5	90.7	87.8	85.9	84.5
110	106.9	93.1	89.7	87.6	86.0
115	111.4	95.5	91.7	89.2	87.5
120	115.9	97.9	93.6	90.9	88.9
125	120.3	100.3	95.6	92.6	90.4
130	124.8	102.7	97.5	94.2	91.8
135	129.2	105.1	99.5	95.9	93.3
140	133.7	107.5	101.4	97.5	94.7
145	138.1	109.9	103.4	99.2	96.2
150	142.6	112.3	105.3	100.9	97.6
155	147.0	114.7	107.2	102.5	99.0
160	151.4	117.1	109.2	104.1	100.5

TABLE XI

BRINE SPRAY POND MODEL DATA FOR VARIOUS WIND VELOCITIES
(Wet Bulb Temperature = 70°F; Dry Bulb Temperature = 75°F;
Droplet Diameter = 2/16"; Salt
Concentration = 20 gm/100 gm)

T_o, °F	T_t, °F				
	0.0 m.p.h.	5 m.p.h.	10 m.p.h.	15 m.p.h.	20 m.p.h.
85	83.2	76.9	76.1	75.7	75.5
90	86.5	77.7	76.5	76.0	75.6
95	89.8	78.5	76.9	76.2	75.8
100	93.0	79.3	77.4	76.5	76.0
105	96.3	80.0	77.8	76.8	76.2
110	99.6	80.8	78.2	77.0	76.4
115	103.0	81.6	78.6	77.3	76.5
120	106.1	82.3	79.0	77.5	76.7
125	109.5	83.1	79.4	77.8	76.9
130	112.7	83.8	79.8	78.0	77.1
135	116.1	84.6	90.3	78.3	77.2
140	119.4	85.3	90.6	78.6	77.4
145	122.7	86.1	91.0	78.8	77.6
150	126.1	86.9	91.5	79.0	77.7
155	129.2	87.5	91.8	79.3	77.9
160	132.6	88.3	92.2	79.5	78.1

TABLE XII

BRINE SPRAY POND MODEL DATA FOR VARIOUS WIND VELOCITIES
(Wet Bulb Temperature = 70°F; Dry Bulb Temperature = 75°F;
Droplet Diameter = 3/16"; Salt
Concentration = 20 gm/100 gm)

T_o, °F	T_t, °F				
	0.0 m.p.h.	5 m.p.h.	10 m.p.h.	15 m.p.h.	20 m.p.h.
85	84.1	79.3	78.1	77.4	77.4
90	88.2	81.0	79.4	78.4	77.8
95	92.4	82.7	80.6	79.4	78.5
100	96.5	84.4	81.8	80.3	79.3
105	100.6	86.2	83.1	81.3	80.1
110	104.6	87.2	84.3	82.2	80.9
115	108.7	89.6	85.5	83.2	81.6
120	112.8	91.3	86.7	84.1	82.4
125	116.7	92.9	87.9	85.1	83.1
130	120.9	94.6	89.2	86.0	83.9
135	125.0	96.3	90.4	86.9	84.6
140	129.0	98.1	91.6	87.9	85.4
145	133.0	99.7	92.8	88.8	86.1
150	137.1	101.4	94.0	89.7	86.9
155	141.0	103.0	95.2	90.6	87.6
160	145.1	104.7	96.6	91.6	88.4

TABLE XIII

BRINE SPRAY POND MODEL DATA FOR VARIOUS WIND VELOCITIES
(Wet Bulb Temperature = 70°F; Dry Bulb Temperature = 75°F;
Droplet Diameter = 4/16"; Salt
Concentration = 20 gm/100 gm)

T_o, °F	T_t, °F				
	0.0 m.p.h.	5 m.p.h.	10 m.p.h.	15 m.p.h.	20 m.p.h.
85	84.5	80.9	79.8	79.1	78.6
90	89.0	83.3	81.7	80.7	80.0
95	93.4	85.7	83.6	82.3	81.4
100	97.9	88.0	85.6	84.0	82.8
105	102.4	90.4	87.5	85.6	84.2
110	106.9	92.8	89.4	87.2	85.7
115	111.3	95.1	91.3	88.8	87.1
120	115.8	97.5	93.2	90.4	88.5
125	120.2	99.8	95.1	92.1	89.9
130	124.6	102.2	97.0	93.7	91.3
135	129.1	104.5	98.9	95.3	92.7
140	133.5	106.9	100.8	96.9	94.0
145	137.9	109.3	102.7	98.5	95.4
150	142.3	111.6	104.5	100.0	96.8
155	146.8	114.0	106.4	101.7	98.2
160	151.2	116.3	108.3	103.3	99.6

TABLE XIV

BRINE SPRAY POND MODEL DATA FOR VARIOUS WIND VELOCITIES
(Wet Bulb Temperature = 70°F; Dry Bulb Temperature = 75°F;
Droplet Diameter = 3/16"; Salt
Concentration = 25 gm/100 gm)

T_o, °F	T_t, °F				
	0.0 m.p.h.	5 m.p.h.	10 m.p.h.	15 m.p.h.	20 m.p.h.
85	84.1	79.2	78.1	77.4	76.9
90	88.2	80.9	79.3	78.3	77.7
95	92.3	82.6	80.5	79.3	78.4
100	96.4	84.3	81.7	80.2	79.2
105	100.5	86.0	82.9	81.2	80.0
110	104.6	87.7	84.1	82.1	80.7
115	108.6	89.4	85.3	83.0	81.5
120	112.7	91.1	86.5	83.9	82.2
125	116.7	92.7	87.7	84.9	83.0
130	120.8	94.4	88.9	85.8	83.7
135	124.8	96.1	90.1	86.7	84.4
140	128.8	97.7	91.3	87.6	85.2
145	132.8	99.4	92.5	88.5	85.9
150	136.9	101.0	93.6	89.4	86.6
155	140.9	102.7	94.8	90.3	87.4
160	104.8	104.3	96.0	91.2	88.0

TABLE XV

PER CENT SPRAY POND EVAPORATION LOSS FOR FRESH WATER AND BRINE WITH VARYING SALT CONCENTRATION
(Wet Bulb Temperature = 70°F;
Dry Bulb Temperature = 75°F;
Orifice Diameter = 1")

T_o, °F	% Evaporation			
	0.0 gm/100 gm	5 gm/100 gm	10 gm/100 gm	15 gm/100 gm
85	2.74887	2.71742	2.68295	2.64511
90	2.75204	2.71742	2.68295	2.64511
95	2.75204	2.71742	2.68295	2.64511
100	2.75204	2.72058	2.68295	2.64511
105	2.75503	2.72058	2.68295	2.64511
110	2.75503	2.72058	2.68594	2.64511
115	2.75503	2.72058	2.68594	2.64511
120	2.75822	2.72378	2.68594	2.64830
125	2.75822	2.72378	2.68913	2.64830
130	2.75822	2.72378	2.68913	2.64830
135	2.76142	2.72677	2.68913	2.65147
140	2.76142	2.72677	2.69230	2.65147
145	2.76458	2.72997	2.69230	2.65147
150	2.76458	2.72997	2.69230	2.65466
155	2.76458	2.73313	2.69230	2.65466
160	2.76777	2.73313	2.69549	2.65466

TABLE XVI

COMPARISON OF SPRAY POND PERFORMANCE DATA
(Nozzle Pressure Drop = 7 psi;
Orifice Diameter = 1 3/16";
Relative Humidity = 70%)

WBT = 64 °F DBT = 60 °F Water Temperature, °F			WBT = 63 °F DBT = 70 °F Water Temperature, °F			WBT = 72 °F DBT = 80 °F Water Temperature, °F		
IN	OUT		IN	OUT		IN	OUT	
	Reported Value	Calculated Value		Reported Value	Calculated Value		Reported Value	Calculated Value
86	71	72	92	77	80.2	107	87	91.7
96	76	75.4	101	81	83.5	116	91	94.1
105	80	80	110	85	86.7	124	94	97.2
114	84	83.8	118	88	89.6	132	97	99.7
123	88	87.6	127	92	92.8			

CHAPTER VII

SUMMARY, CONCLUSIONS, AND RECOMMENDATIONS

7.1 Summary and Conclusions

A mathematical model that simulates the cooling process involved in a spray cooling system has been presented. The model was first solved for fresh water, simulating the conditions for which performance data was available. Values were assumed for R/r_o and relative humidity which yielded the closest fit to the published data. A parametric analysis was then performed to establish curves that could be used for designing spray cooling systems.

Having established optimum values for R/r_o and relative humidity for fresh water using published data, salt water then was analyzed. Calculations were performed using the thermodynamic properties of salt water. The following observations were made concerning the results generated with this model.

1. Results obtained through the proposed model compare favorably with published data. The model can be used to predict the effect of spray cooling over a wide range of prevailing conditions.
2. The proposed mathematical model involves most of the significant variables influencing the design of spray ponds. This model provides an accurate and efficient approximation to solve

problems related to spray ponds. Since it is based on theoretical as well as established empirical relations, it should be quite useful for extending predictions in design work.

3. The results of this study indicate that a greater cooling effect is achieved by the smaller initial droplet diameters, due to the increase in the cooling surface area. The increase in wind velocity also provides a larger cooling effect due to the increase of air circulation around the spray droplets.
4. The water loss due to evaporation is very small while the loss is slightly less for brine than for fresh water.
5. The presence of NaCl in water droplets increases the cooling somewhat over fresh water. These results may be encouraging for localities where only sea water is available for cooling, and where damage by wind blown brine droplets could be tolerated on the land adjacent to the spray pond.
6. The range of variables used in the design of cooling spray ponds are listed in Table XVII [3]. The proposed model very closely predicts the experimental data available in this design range. Any further extension of the variables beyond the range specified in Table XVII should be verified with experimental data.

7.2 Recommendation for Further Work

Additional work is recommended to extend the range of applicability of the model developed in this study, and to provide additional

TABLE XVII

SPRAY POND ENGINEERING DATA AND DESIGN

Parameters	Recommendations		
	Usual	Minimum	Maximum
Nozzle Capacity, gal/min. each	35-50	10	60
Height of Nozzles Above Sides of Basin, ft.	7-8	2	10
Nozzle Pressure, lb/sq.in.	5-7	4	10
Size of the Nozzle and Nozzle Arms	2	1¼	2½
Depth of Pond Basin, ft.	4-5	2	7
Wind Velocity, m.p.h.	5	3	10

verification on the validity of the model application to brine. Specifically, additional work needs to be done in the following areas:

1. In order to verify results obtained herein, an experimental study should be undertaken. A spray system could be built in a controlled environment test chamber that could be used to simulate a wide range of prevailing weather conditions. The effect of various parameters on the spray cooling system could be measured. By comparing experimental results to those predicted mathematically, better values can be established for experimental coefficients appearing in the mathematical model.
2. An extension of this study to include the evaluation of cooling towers to cool and aerate brine is recommended.

BIBLIOGRAPHY

(1) Diluzio, Frank C. "Water Use and Thermal Pollution." Power Engineering (June, 1968).

(2) Zung, Joseph T. "Evaporation Rate and Lifetimes of Clouds in Air --The Cellular Model." The Journal of Chemical Physics, Vol. 46 (1967), p. 2064.

(3) Chemical Engineer's Handbook, Fourth Edition. New York: McGraw-Hill Book Company, 1960, pp. 15-21.

(4) Dufour, L., and R. Defay. Thermodynamics of Clouds. New York: Academic Press, Inc., 1963.

(5) Ranz, W. D., and W. R. Marshall. "Evaporation from Drops." Chemical Engineering Progress, Vol. 48 (1952), pp. 141, 173.

(6) Chemical Engineer's Handbook, Fourth Edition. New York: McGraw-Hill Book Company, 1960, pp. 18-67.

(7) Marshall, W. R., Jr. "Atomization and Spray Drying." Chemical Engineering Progress Monograph Series, No. 2, Vol. 50 (1954), p. 61.

(8) Mayer, W. E., and W. E. Ranz. "Encyclopedia of Chemical Technology." The Interscience Encyclopedia, Inc., Volume 12, New York (1954), p. 704.

(9) Chou, James C. S., and Allen M. Rowe, Jr. "Enthalpies of Aqueous Sodium Chloride Solutions from 32 to 350° F." Desalination, Vol. 6 (1969), pp. 105-115.

(10) Rowe, Allen M., Jr., and James C. S. Chou. "Pressure-Volume-Temperature-Concentration Relation of Aqueous NaCl Solutions." Journal of Chemical and Engineering Data, Vol. 15, No. 1 (1970), p. 61.

(11) Dorsey, N. E. Properties of Ordinary Water Substance. New York: Reinhold Publishing Corporation, 1940, p. 73.

(12) "Heating, Ventilating, Air Conditioning Guide," 38th Edition. American Society of Heating, Refrigerating, and Air Conditioning Engineers (1960), p. 598.

(13) Kays, W. M. Convective Heat and Mass Transfer. New York: McGraw-Hill Book Company, 1966.

(14) Chou, James C. S. "Thermodynamic Properties of Aqueous Sodium Chloride Solutions from 32 to 350 F." (unpublished Ph.D. Dissertation, Oklahoma State University, Stillwater, Oklahoma, 1968.)

(15) Saline Water Conversion Engineering Data Book. U. S. Government Printing Office, 1965, pp. 11-95.

(16) Maxwell, J. C. Collected Scientific Papers. Cambridge, Ill. (1890), 626.

(17) Langmuir, I. "The Dissociation of Hydrogen into Atoms." The Journal of the American Chemical Society, Vol. 37 (1915), p. 417.

(18) Schäfer, K. "Verdamphungserscheinungen an Quecksilbertröphchen." Zeitschrift Für Physik, 77 (1932), 198.

(19) Welander, P. "On the Temperature Jump in a Rarefied Gas." Arkiv Für Fysik, 7 (1954), 507.

(20) Fuchs, N. A. "Evaporation and Droplet Growth in Gaseous Media." New York: Pergamon Press, Inc., 1959.

(21) Schäfer, K., and W. Rating. "Über den Einflub des gehemmten Austauschs der Translations-und Schwingungsenergie auf des Warmeleitvermögen der Gase." Annalen Der Physik, 42, (1942), 176.

(22) Okuyama, M., and J. T. Zung. "Evaporation-Condensation Coefficient for Small Droplets." The Journal of Chemical Physics, Vol. 46 (1967), p. 1580.

(23) Frisch, H. L., and R. C. Collins. "Diffusional Processes in the Growth of Aerosol Particles." The Journal of Chemical Physics, Vol. 21 (1958), p. 2158.

(24) Mason, B. G. "Spontaneous Condensation of Water Vapor in Expansion Chamber Experiment." The Proceedings of the Physical Society, Vol. 64B (1951), p. 773.

(25) Schlichting, Hermann. Boundary-Layer Theory. Sixth Edition. New York: McGraw-Hill Book Company, 1968.

(26) Carslaw, H. S. Conduction of Heat in Solids. New York: Oxford University Press, Inc., 1959.

(27) Reiss, Howard, and Victor K. LaMer. "Diffusional Boundary Value Problems Involving Moving Boundaries, Connected with the Growth of Colloidal Particles." The Journal of Chemical Physics, Vol. 18 (1950), p. 1.

(28) Kronig, R., and J. Bruijsten. "On the Theory of the Heat and Mass Transfer from a Sphere in a Flowing Medium at Low Values of Reynolds Number." Applied Science Research, Vol. A2 (1951), p. 439.

APPENDIX A

QUASI-STATIONARY EVAPORATION OF DROPLETS MOTIONLESS RELATIVE TO THE MEDIUM

The purpose of this appendix is to present a literature survey concerned with the evaporation of droplets of a pure liquid. Published results evaluating the influence of concentration change and temperature change at the droplet surface on the rate of evaporation are also presented.

This appendix deals with the simplest case of evaporation where the droplet is motionless relative to the medium and where hydrodynamic factors are absent. Most work in this area has been developed for quasi-stationary, motionless droplets. As will be shown in Appendix D the non-stationary evaporation can, in many cases, be treated as quasi-stationary to a very close approximation.

A.1 The Maxwell Equation

The theory of evaporation of droplets in a gaseous medium was first developed by Maxwell [16]. He considered the simplest case, that of stationary evaporation from a spherical droplet, motionless relative to an infinite, uniform medium. He assumed that the vapor concentration at the surface of the drop was equal to its equilibrium concentration C_o (i.e., the concentration corresponding to the vapor pressure at the temperature of the droplet for the case of intermediate sized droplets).

As will be shown, this assumption is true when the radius of the drop is significantly greater than the mean free path of the vapor molecules.

For this case of stationary evaporation, the rate of diffusion of the vapor of the droplet across any spherical surface with radius r and concentric with the drop is constant and express by the equation

$$I = - 4\pi r^2 \frac{dC}{dr} D \quad gm.sec^{-1} \tag{A.1}$$

where

I = rate of evaporation of droplet,

D = diffusion coefficient of the vapor, and

C = vapor concentration (gm cm^{-3}).

Integration of Equation (A.1) gives

$$C = \frac{1}{4\pi r D} + \text{Constant} \quad . \tag{A.2}$$

If C_∞ is the concentration of vapor at infinite distance from the drop, the following boundary condition can be obtained

$$C = C_\infty \quad \text{at} \quad r = \infty \quad . \tag{A.3}$$

And, according to the above assumption

$$C = C_o \quad \text{at} \quad r = r_o$$

where r_o is the radius of the droplet.

From condition (A.3), it follows that

$$C - C_\infty = \frac{I}{4\pi r D} \tag{A.4}$$

which results in the following expression:

$$(I_o \equiv I) = 4\pi r_o D (C_o - C_\infty) \tag{A.5}$$

where,

I_o = rate of evaporation of droplet from Maxwell's equation.

The rate of evaporation of a drop for condition (A.3) is, therefore, completely determined by the rate of diffusion of the vapor in the medium, i.e., diffusion controls the rate of evaporation. Equation (A.5) shows that in the case under consideration, the rate of evaporation of a droplet in a gaseous media is not proportional to the surface area of the droplet as in evaporation into a vacuum (i.e., purely kinetic control), but to the radius of the droplet.

In deriving Equation (A.5), Maxwell recognized the mathematical analogy between the theory of stationary evaporation and potential theory (potential being replaced by vapor concentration in the former). This analogy holds because the differential equations have the same form.

In applying Equation (A.5) to evaporation, he assumed that the vapor obeys the ideal gas laws and thus the vapor concentration has the following form:

$$C = \frac{PM}{RgT} . \tag{A.6}$$

Equation (A.5) then becomes

$$I = \frac{4\pi r_o DM (P_o - P_\infty)}{RgT} \tag{A.7}$$

where,

M = the molecular weight of the evaporating substance.

Strictly speaking, the evaporation of a droplet cannot be a stationary process since the radius and hence, the rate of evaporation, is constantly decreasing. But for $C_o \ll \rho$ (where ρ is the density of

the droplet), it can be assumed that the rate of evaporation at a given moment can be expressed by Equation (A.5).

Under steady state conditions, the rate of evaporation can be determined from the following equation:

$$I = -\frac{dm}{dt} \tag{A.8}$$

where,

$m = \frac{4}{3} \rho \pi r^3$, and

t = time.

Equation (A.5) can then be rewritten in the form

$$-\frac{d(r^2)}{dt} = \frac{2D}{\rho} (C_o - C_\infty) \tag{A.9}$$

or

$$-\frac{dS}{dt} = \frac{8 \pi D}{\rho} (C_o - C_\infty) \tag{A.10}$$

where,

$S = 4 \pi r^2$ = droplet surface.

Integration of Equations (A.9) and (A.10) give:

$$r_o^2 - r^2 = \frac{2D}{\rho} (C_o - C_\infty)t \tag{A.11}$$

or

$$S_o - S = \frac{8 \pi D}{\rho} (C_o - C_\infty)t \tag{A.12}$$

where r_o and S_o are the initial radius and surface area of the droplet, respectively. The surface area of the droplet is thus a linear function of time.

From Equations (A.1) and (A.5) it follows that

$$C - C_\infty = \frac{r_o}{r} (C_o - C_\infty) \quad . \tag{A.13}$$

This equation will be used in Appendix B.

A.2 Influence of the Concentration Change at the Surface on the Rate of Evaporation

In 1915, Langmiur [17] pointed out that there exists a rapid change in vapor concentration at the surface of an evaporating droplet which was not considered in Maxwell's work. The necessary correction to Maxwell's equation for this effect was first derived by Schafer in 1932 [18].

The effect of concentration change on the rate of evaporation can be calculated to a first approximation by assuming that the solution to Fick's equation as well as Equation (A.13) are valid only at a distance greater than $\Delta \approx 1$ (the mean free path of the gas molecule) from the surface of the droplet [19]. It is also assumed that in the layer of thickness Δ adjacent to the surface, the interchange of vapor molecules proceeds unhindered as in a vacuum [20]. The rate of evaporation from a droplet in a vacuum equals $4\pi r^2 C_o \nu \alpha$, where $\nu = (kT/2\pi m)^{1/2}$ and is one-fourth of the mean absolute velocity of the vapor molecules (the parameter α is the vaporization constant of the liquid). Then, the rate of evaporation from the droplet is given by

$$I = 4\pi r^2 (C_o - C_1) \nu \alpha \qquad (A.14)$$

where C_1 is defined as the vapor concentration at distance Δ from the droplet. This rate equals the rate of evaporation to the surrounding space by diffusion, and is

$$I = - 4\pi r^2 D \frac{dC}{dr} \quad . \qquad (A.15)$$

According to the above assumption, Equation (A.13) is correct when $r > r_o + \Delta$, and results in:

$$\left(\frac{dC}{dr} = -\frac{C}{r}\right)_{r=r_o+\Delta} = -\frac{C_1}{r+\Delta} \quad . \tag{A.16}$$

Equation (A.15) becomes

$$I = 4\pi(r+\Delta)DC_1 \quad . \tag{A.17}$$

It follows from Equations (A.14) and (A.17) that

$$C_1 = (r^2 C_o \nu\alpha)/[r^2 \nu\alpha + D(r+D)] \tag{A.18}$$

$$I = \frac{I_o}{\frac{D}{r\nu\alpha} + \frac{r}{r+\Delta}} \quad . \tag{A.19}$$

Equation (A.19) [Fuch's equation] with Δ equal 1 (mean free path of vapor molecule) gives a slightly low value for the diffusion rate I. To obtain the correct value of I, one must take $\Delta = \beta 1$ where β is a factor greater than one [21].

Equation (A.19) is valid for small droplets having a radius less than 10^{-2} cm. Recently, a correction term to Equation (A.19) has been suggested by Zung and Okuyama [22] for the evaporation rate of droplets having radii down to 10^{-8} cm. The combined Fuchs-Zung-Okuyama equation is written as follows:

$$I = \frac{4\pi r D(C_o - C_\infty)}{\frac{D}{r\nu\alpha\Phi} + \frac{r}{r+\Delta}} \tag{A.20}$$

where,

$\Phi = \mathrm{Exp}\left(-\frac{3\nu\sigma}{rkT}\right)$,

σ = surface tension of the droplet,

$\nu = \left(\frac{kT}{2\pi m}\right)^{1/2}$, and

$$\Delta = \frac{2D}{(8kT/\pi m)^{1/2}} \quad .$$

Frisch and Collins [23] have suggested that a change in the droplet radius may affect such parameters as surface tension of the droplet which in turn would change the value of α. Also, a change in droplet radius would cause a change in temperature since the heat absorbed or liberated would affect the evaporation coefficient α.

A.3 The Fall in Temperature of Free Evaporating Droplets

In Maxwell's article [16], an equation was also derived for the decrease in temperature of the droplet caused by evaporation. He neglected heat transfer by convection and radiation, and assumed that the conductivity of the gaseous media (k_a) is independent of the temperature and concentration of vapor (assume k_a is constant); then the analogy between heat conductivity and diffusion allowed him to derive an equation for the stationary distribution of temperature around a spherical droplet, analogous to (A.13)

$$T_\infty - T = \frac{r_o}{r}(T_\infty - T_o) \qquad (A.21)$$

where T_∞ is the temperature at an infinite distance from the droplet (temperature of the medium) and T_o is the temperature at the surface of the droplet. An equation analogous to (A.5) may be obtained for the heat flux to the drop from the surrounding space due to the conductivity of the medium as

$$Q = 4\pi r k_a (T_\infty - T_o) \quad \text{cal sec}^{-1} \quad . \qquad (A.22)$$

In this study, following the procedure of Maxwell, the following relation was derived. In stationary evaporation, the quantity of heat transferred to the droplet or from the droplet is equal to the amount lost in evaporation. Hence,

$$Q = IL \quad \text{cal sec}^{-1} \tag{A.23}$$

and

$$T_\infty - T_o = \frac{LD}{k_a}(C_o - C_\infty) \tag{A.24}$$

where L is the latent heat of evaporation of the liquid as shown in Figure 17.

Inserting Equation (A.6) into Equation (A.24), it follows that

$$T_\infty - T_o = \frac{LDM}{Rg\, k_a}\left(\frac{P_o}{T_o} - \frac{P_\infty}{T_\infty}\right) \quad . \tag{A.25}$$

When $(T_\infty - T_O)$ is small, this problem can be solved algebraically, using the Clausius-Clapeyron equation [24] as shown in Chapter IV.

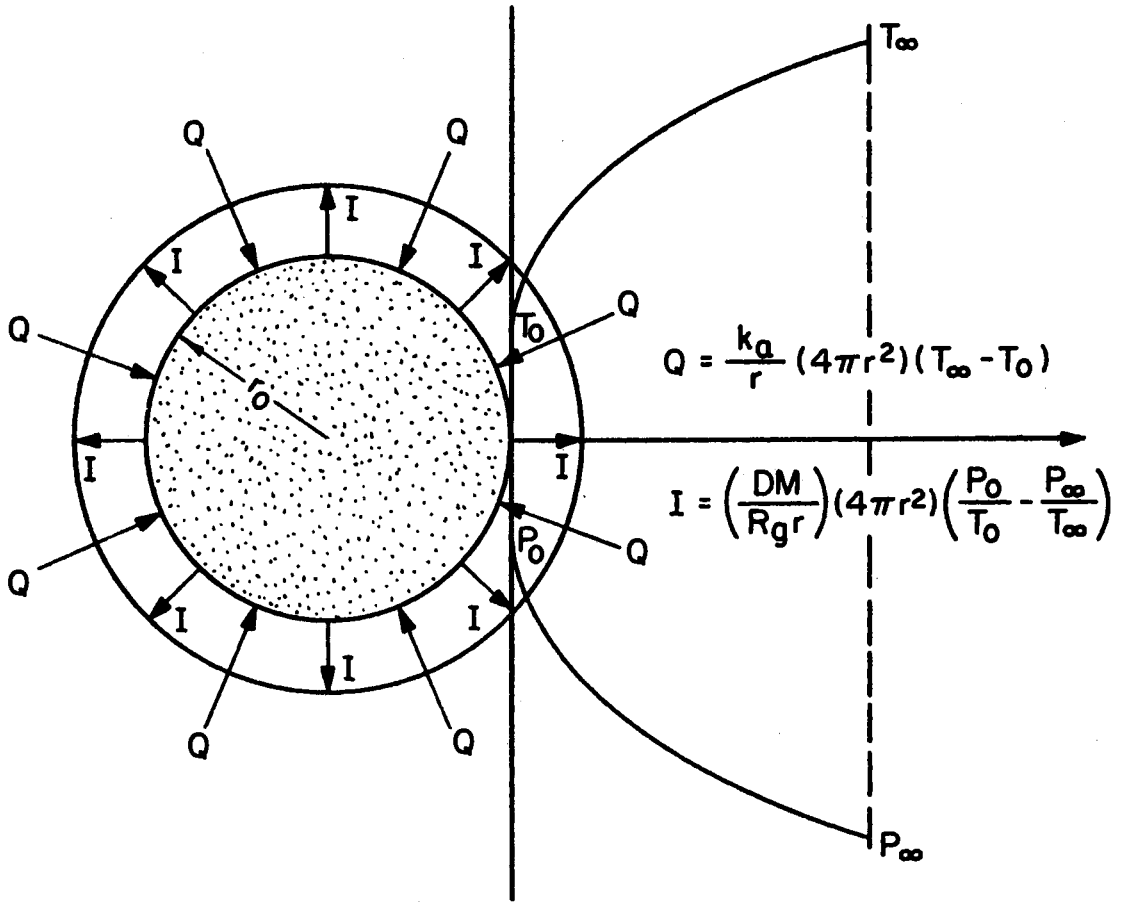

Figure 17. Idealization of Droplet Evaporating in Still Air; Evaporation and Heat Transfer Occur Uniformly At All Points On The Drop Surface

APPENDIX B

NON-STATIONARY EVAPORATION OF DROPLETS MOTIONLESS RELATIVE TO THE MEDIUM

The purpose of this appendix is to present the effect of decrease in size of the evaporating droplet on the rate of evaporation.

First, consider the growth of a droplet in an infinite supersaturated medium [20]. If the process is quasi-stationary, the concentration distribution of the vapor is expressed by Equation (A.13)

$$C_\infty - C = \frac{r_o}{r} (C_\infty - C_o) \tag{B.1}$$

and is represented by Curve A in Figure 18.

When the radius of the droplet increases by Δr, the quasi-stationary concentration distribution is then given by Curve B. The real distribution deviates from the quasi-stationary distribution and is represented by a curve such as C.

Figure 18 shows that the concentration gradient at the surface of the growing droplet and consequently the rate of evaporation is slightly greater than for the quasi-stationary case. For a rough estimation of this effect, it was assumed that the concentration distribution is given by the equation

$$C_\infty - C = \frac{r_o}{r} (C_\infty - C_o) \Psi(r) \tag{B.2}$$

where the correction factor Ψ is only a function of r, and r is function of time.

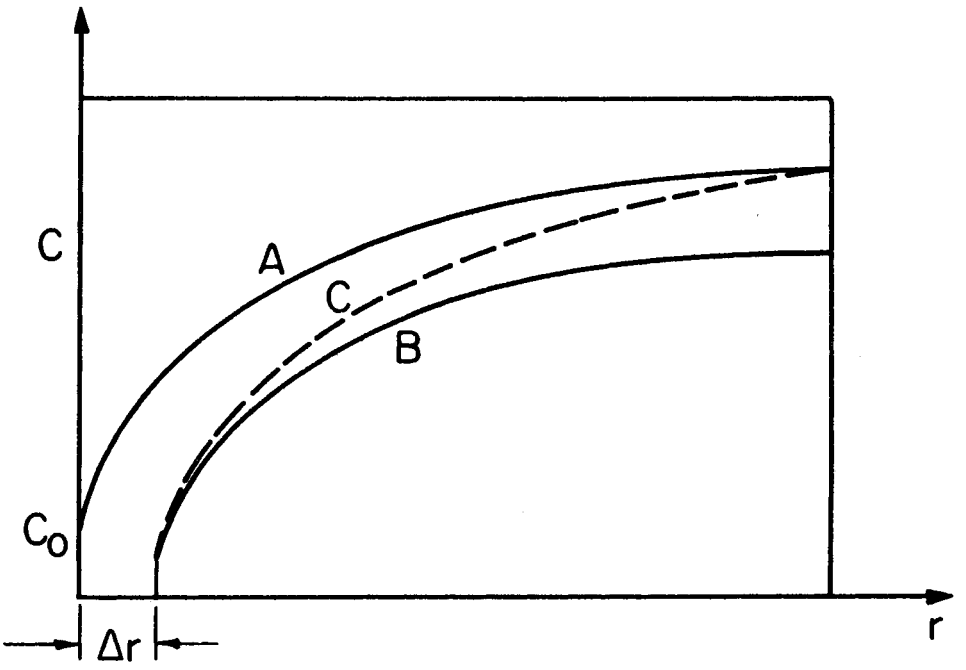

Figure 18. Quasi-Stationary (Solid Line) and Real (Broken Line) Distributed of Vapor Concentration Near a Growing Droplet

The equation of diffusion in a non-stationary motionless medium is given by

$$\frac{\partial C}{\partial t} = D\left(\frac{\partial^2 C}{\partial r^2} + \frac{2}{r}\frac{\partial C}{\partial r}\right) \quad . \tag{B.3}$$

Equations (B.2) and (B.3) give

$$\Psi \frac{\partial r}{\partial t} = Dr \frac{\partial^2 \Psi}{\partial r^2} \quad . \tag{B.4}$$

It was assumed for simplicity that $\left(\frac{\partial r}{\partial t}\right)/r$ is constant over a short period of time. Letting $\left(\frac{\partial r}{\partial t}\right)/Dr = \beta^2$, Equation (B.4) can be written as:

$$\frac{\partial^2 \Psi}{\partial r^2} = \beta^2 \Psi \tag{B.5}$$

whence on integration and remembering that $\Psi = 1$ at $r = r_o$,

$$\Psi = \exp\left[-\beta(r - r_o)\right] \quad . \tag{B.6}$$

For a general solution the term with $e^{+\beta r}$ can be omitted, since $e^{+\beta r} \to \infty$ as $r \to \infty$. From Equations (B.2) and (B.3), it follows that

$$\left(\frac{\partial C}{\partial r}\right)_{r=r_o} = (C_\infty - C_o)\left(\frac{1}{r_o} + \beta\right) \quad . \tag{B.7}$$

Thus,

$$\begin{aligned} I &= I_o(1 + \beta r_o) \\ &= I_o\left(1 + \sqrt{\frac{r\left(\frac{dr}{dt}\right)}{D}}\right) \end{aligned} \tag{B.8}$$

where I_o is the rate of growth of the droplet for the quasi-stationary process.

Since $4\pi\rho r^2 \frac{dr}{dt} = 4\pi r D/(C_\infty - C_o)$, the following expression can be obtained:

$$I = I_o \left(1 + \sqrt{\frac{C_\infty - C_o}{\rho}}\right) \quad . \tag{B.9}$$

In evaporation, rather than condensation which is treated above, the effect is the opposite. The real rate of evaporation is slightly lower for the quasi-stationary case and a minus sign must be placed before the root in Equation (B.9).

APPENDIX C

QUASI-STATIONARY EVAPORATION OF DROPLETS MOVING RELATIVE TO THE MEDIUM

In this appendix the dimensionless numbers which were used in the model calculation are presented. The correction to the rate of evaporation equations due to the change in concentration are also presented [Equation (C.9)].

C.1 Reynolds Number

The Reynolds number is defined as:

$$Re \equiv \frac{2V_o r}{\nu} \quad . \tag{C.1}$$

V_o is the gas velocity far from the droplet, while ν is the kinematic viscosity of the medium, and r is the droplet radius. The magnitude of this number determines whether the motion is turbulent or laminar.

C.2 Nusselt Number

$$Nu \equiv \frac{2rQ}{k_a S (T_\infty - T_o)} \tag{C.2}$$

Q is the amount of heat transferred to the droplet in a unit time, S is the surface area of the droplet, k_a is the thermal conductivity of the medium, and $(T_\infty - T_o)$ is the difference in temperature between the medium and the droplet.

C.3 Sherwood (or Nusselt Diffusion) Number

The Sherwood number is defined as:

$$Sh = \frac{2rI}{D\,S\,(C_o - C_\infty)} \tag{C.3}$$

I is the rate of evaporation of the droplet in the stream.

C.4 Prandtl Number

The Prandtl number is defined as:

$$Pr = \frac{\nu}{\alpha} \tag{C.4}$$

where $\alpha \equiv \frac{k_a}{\rho_a C_p}$, the thermal diffusivity. The kinematic viscosity is a diffusivity for momentum, or for velocity, in the same sense that the thermal diffusivity is a diffusivity for heat, or for temperature. If the Prandtl number is 1, then heat and momentum are diffused through the fluid at the same rate.

C.5 Schmidt (or Prandtl Diffusion) Number

The Schmidt number is defined as:

$$Sc = \frac{\nu}{D} \tag{C.5}$$

which is similar to the Prandtl number, except that it accounts for the effect of diffusion.

For a spherical droplet:

$$Nu = \frac{Q}{2\pi r_o k_a (T_\infty - T_o)}\ , \text{ and} \tag{C.6}$$

$$Sh = \frac{I}{2\pi r_o D (C_o - C_\infty)}\ . \tag{C.7}$$

Using the principle of similarity, one can show that Nu is a function of Reynolds number and Prandtl number, and that the Sherwood number is a function of the Reynolds number and the Schmidt number.

The Prandtl number and Schmidt number usually have a value of the order 1 [13]; (under normal conditions) $Pr \simeq 0.7$ in air and $Sc \simeq 0.7$ for water vapor in air [13].

There should exist a diffusion boundary layer, where the vapor concentration falls from C_o at the surface of the sphere to the concentration in the stream C_∞. Because of the analogy between the equations for viscous liquid motion and convective diffusion when the kinematic viscosities and diffusivities are similar; i.e., when $Sc \simeq 1$, the thickness of the diffusion boundary layer δ' and rate boundary layer δ are also similar. The same applies to the thickness δ'' of the temperature boundary layer resulting from heat transfer from a ventilated body. Here it was assumed that $\delta'' = \delta$.

By using the similarity principle, it can be shown that for the case of this study, the rate of evaporation or heat transfer is proportional to $(Re)^{1/2}$. Similar considerations also lead to the same results. $\delta/r = \beta\ Re^{-1/2}$, where β increases from 0.3 at the forward stagnation point to 0.8 at the break away point [25]. Hence, δ' is also proportional to $Re^{-1/2}$ and the rate of evaporation is consequently proportional to $Re^{1/2}$.

The magnitude of the effect of the change in vapor concentration at the surface of a droplet on its rate of evaporation depends on the ratio of the mean free path of the vapor molecules to the thickness of diffusion boundary layer δ'. Following the same line of reasoning as presented in part 2 of Appendix A, and noting that at high Re, $\delta \ll r$,

the surface of the droplet can be considered flat. The following expression applies to this case:

$$I_f = I_{fo}\left[1 + \frac{D}{\nu\,\alpha(\delta' - \Delta)}\right]^{-1} \quad . \tag{C.8}$$

The parameter I_{fo} is the rate of evaporation in the absence of a concentration change. It is easily seen that $\delta' = \frac{2r}{Sh}$. By replacing Δ with $\beta 1$ (part 2, Appendix A), Equation (C.8) can be rewritten

$$I_f = I_{fo}\left[1 + \frac{D}{\nu\,\alpha\left(\frac{2r}{Sh} - \beta 1\right)}\right]^{-1} \quad . \tag{C.9}$$

The correction for the concentration change has practical significant only for liquids with small α (vaporization constant). The term $\beta 1$ in Equation (C.9) is small when compared to $\frac{2r}{Sh}$. For this case, it can be demonstrated with boundary layer theory that this term can be neglected.

APPENDIX D

RATE OF EVAPORATION

In this appendix the rate of evaporation equation which was used in the energy and mass balance equations is presented. The rate of evaporation is presented for two ranges of the Reynolds number (Re $\ll$ 1, and Re $>$ 1) to evaluate the effect of wind velocity.

D.1 Evaporation Rate for Reynolds Number Much Less Than One

This section contains solutions for both the non-stationary and quasi-stationary evaporation.

D.1.1 Non-Stationary Evaporation of Droplets, Assuming Zero Wind Velocity

The equation of diffusion for a non-stationary motionless medium is given by

$$\frac{\partial C}{\partial t} = D\left(\frac{\partial^2 C}{\partial r^2} + \frac{2}{r}\frac{\partial C}{\partial r}\right) \tag{D.1}$$

with boundary conditions:

$$\left.\begin{aligned} C &= C_o \qquad r = r_o \\ \frac{\partial C}{\partial r} &= 0 \qquad r = R \end{aligned}\right\} \quad . \tag{D.2}$$

Assuming the initial concentration is zero, the exact solution of Equation (D.1) with its appropriate boundary conditions, is given by Carslaw and Jaeger [26]. A simpler solution to Equation (D.1) has also been given by Reiss and LaMer [27] in their study on the growth rate of a droplet as given by Fuchs' expression [20]:

$$I = 4\pi r_o D C_o \text{Exp}\left[\frac{-3 r_o D t}{(R - r_o)^3}\right] . \qquad (D.3)$$

Equation (D.3) is valid only when $r/R \leq 0.1$ and $t \gg R/20D$ which is the most practical case.

It is to be noted that the highest value of the term t in Equation (D.3) is the saturation exposure time, t_s.

However, Equation (D.3) can also be obtained by assuming that evaporation is quasi-stationary. Let C_t be the vapor concentration at time (t) at a sufficiently great distance from the droplet (where the concentration can be considered independent of r). Then, where $r/R \leq 0.1$, it can be assumed to a close approximation that the total mass of vapor in the cell at time (t) is

$$M \simeq \frac{4}{3}\pi (R - r_o)^3 C_t \qquad (D.4)$$

while the quasi-stationary rate of evaporation at time (t) is

$$I = 4\pi r_o D (C_o - C_t) \qquad (D.5)$$

since,

$$I = -\frac{dM}{dt}$$

$$r_o D (C_o - C_t) = -\frac{1}{3} (R - r_o)^3 \frac{dC_t}{dt} . \qquad (D.6)$$

Integrating Equation (D.6) with the same initial conditions as Equation (D.1) (initial concentration is zero) leads to

$$\frac{C_o - C_t}{C_o} = \text{Exp}\left[\frac{-3r_o D t}{(R - r_o)^3}\right] .$$

The rate of evaporation, I, becomes:

$$I = 4\pi r_o D(C_o - C_t)$$

$$= 4\pi r_o C_o D \text{Exp}\left[\frac{-3r_o D t}{(R - r_o)^3}\right] \qquad (D.7)$$

which is the same as Equation (D.3).

Thus, the rate of evaporation for this case can be assumed, to a close approximation, to be the same as for the quasi-stationary case as long as $r_o/R \leq 0.1$ and $t \gg R/20D$.

D.1.2 Quasi-Stationary Cooling and Evaporation of Droplets Moving Relative to the Medium

The equation of diffusion in a quasi-stationary moving medium is given by:

$$D\nabla^2 C - U \cdot \text{grad } C = 0 \qquad (D.8)$$

where,

$U \equiv$ velocity vector of the medium, and

∇^2 = Laplace operator.

It applies when the medium is homogeneous and the diffusion coefficient does not depend on the concentration of the diffusing substance.

The boundary conditions are:

$$\left.\begin{aligned} C &= C_o \qquad r = r_o \\ C &= 0 \qquad r = \infty \end{aligned}\right\} \quad . \tag{D.9}$$

Equation (D.8) with the above boundary conditions was solved by perturbation methods by Kronig and Bruijsten [28]. Their solution is:

$$C' = \frac{1}{r'} + \epsilon\left[\frac{1}{2r'} + \cos\theta\left(\frac{-3}{4r'} + \frac{3}{8r'^2} - \frac{1}{8r'^3}\right) - \frac{1}{2}(1 - \cos\theta)\right] \tag{D.10}$$

where,

$C' = \dfrac{C}{C_o}$,

$r' = \dfrac{r}{r_o}$,

$\epsilon = \dfrac{1}{2}\,Re \cdot Sc$, and

r, θ = polar coordinates in space.

The concentration gradient at the surface of the droplet is given by:

$$\left(\frac{\partial C'}{\partial r'}\right)_{r'=1} = \left[-1 + \epsilon\left(-\frac{1}{2} + \frac{3}{8}\cos\theta\right)\right] \quad . \tag{D.11}$$

The rate of evaporation, I_f, is given by:

$$I = -D\int\left(\frac{C_o}{r_o}\right)\left(\frac{\partial C'}{\partial r'}\right)_{r'=1} dS \tag{D.12}$$

$$= -D\frac{C_o}{r_o}\int_o^{\pi}\int_o^{2\pi}\left[-1 + \epsilon\left(-\frac{1}{2} + \frac{3}{8}\cos\theta\right)\right] \times r_o^2 \sin\theta\, d\theta\, d\Phi$$

$$= 4\pi D C_o r_o \left(1 + \frac{\epsilon}{2}\right) \tag{D.13}$$

and the Sherwood (or Nusselt diffusion) number, Sh, is given by:

$$Sh = \frac{2r_o \times I_f}{4\pi r_o^2 D (C_o - 0)}$$

$$= 2\left(1 + \frac{\epsilon}{2}\right)$$

$$= 2\left(1 + \frac{Re \times Sc}{4}\right) \quad . \qquad (D.14)$$

D.2 Evaporation Rate for Reynolds Numbers Greater Than One

At larger value of Reynolds number (Re > 1), following the majority of the workers in this field, it has been assumed that the convection term in the mass and energy balance equations can be evaluated by using Ranz and Marshall's equation [5], where the Sherwood (or Nusselt diffusion) number is given by

$$Sh = 2[1 + 0.3 (Re)^{1/2} (Sc)^{1/3})] \qquad (D.15)$$

and

$$I = 4\pi r_o D [1 + .03 (Re)^{1/2} (Sc)^{1/3}](C_o - C_\infty) \quad . \qquad (D.16)$$

VITA

Asem M. Elgawhary

Candidate for the Degree of

Doctor of Philosophy

Thesis: SPRAY POND MATHEMATICAL MODEL FOR COOLING FRESH WATER AND BRINE

Major Field: Mechanical Engineering

Biographical:

Personal Data: Born October 15, 1941, in Fakous, Egypt, the son of Mr. and Mrs. Mohamed Elgawhary.

Education: Graduated from Cairo University, Egypt in June, 1963, with the Bachelor of Science degree in Mechanical Engineering; received the Master of Science degree in Mechanical Engineering from Oklahoma State University in August, 1969; completed the requirements for the Doctor of Philosophy degree at Oklahoma State University in July, 1971.

Professional Experience: Employed as an instructor in Cairo Higher Industrial Institute, Egypt, from October, 1963, to March, 1968; technical specialist with Denver Research Institute, Colorado, Summer 1968; graduate teaching and research assistant, School of Mechanical and Aerospace Engineering, Oklahoma State University, 1968-1971.

Professional Societies: Member, The Egyptian Society of Engineers, Cairo, U. A. R.